Discretized light-cone quantization and the effective interaction in hadrons

Hans-Christian Pauli
Max-Planck-Institut für Kernphysik
D-69029 Heidelberg

30 August 1999

Abstract

Light-cone quantization of gauge theories is discussed from two perspectives: as a calculational tool for representing hadrons as QCD bound-states of relativistic quarks and gluons, and as a novel method for simulating quantum field theory on a computer. A general non-perturbative method for numerically solving quantum field theories, 'discretized light-cone quantization', is outlined. Both the bound-state spectrum and the corresponding relativistic wavefunctions can be obtained by matrix diagonalization and related techniques. Emphasis is put on the construction of the light-cone Fock basis and on how to reduce the many-body problem to an effective Hamiltonian. The usual divergences are avoided by cut-offs and subsequently removed by the renormalization group. For the first time, this programme is carried out within a Hamiltonian approach, from the beginning to the end. Starting with the QCD-Lagrangian, a regularized effective interaction is derived and renormalized, ending up with an almost solvable integral equation. Its eigenvalues yield the mass spectrum of physical mesons, its eigenfunctions yield their wavefunctions including the higher Fock-space components. An approximate but analytic mass formula is derived for all physical mesons.

Preprint MPIH-V19-1999
60 pages, 13 figures, 11 tables, 41 references
PACS-Index: 11.10Ef, 11.15Tk, 12.38Lg, 12.40Yx
Better figure quality is obtained from .uu and .ps files from
ftp anonymous@franny.mpi-hd.mpg.de/pub/pauli/99korea/

To be published in:
New Directions in Quantum Chromodynamics, C.R. Ji, *Ed.,*
American Institute of Physics, New York, 1999.
(Proceedings of a Summer School in Seoul, Korea, 26 May - 18 June 1999.)

Contents

1 Introduction

One of the outstanding problems in particle physics is the determination of the structure of hadrons such as the proton and neutron in terms of their fundamental quark and gluon degrees of freedom. Over the past twenty years two fundamentally different pictures have developed. One, the constituent quark model is closely related to experimental observation. The other, quantum chromodynamics is based on a covariant non-abelian quantum field theory. The front form (also known as light-cone quantization) appears to be the only hope of reconciling these two. This elegant approach to quantum field theory is a Hamiltonian gauge-fixed formulation that avoids many of the most difficult problems in the conventional equal-time formulation of the theory.

The natural gauge for light-cone Hamiltonian theories is the light-cone gauge $A^+ = 0$. In this physical gauge the gluons have only the two physical transverse degrees of freedom. One imagines that there is an expansion in multi-particle occupation number Fock states. But even in the case of the simpler abelian quantum theory of electrodynamics very little is known about the nature of the bound state solutions in the strong-coupling domain. In the non-abelian quantum theory of chromodynamics a calculation of bound-state structure has to deal with many difficult aspects simultaneously. Confinement, vacuum structure and chiral symmetry inter-twine with the difficulties of describing a (relativistic) many-body system and the non-perturbative renormalization of a Hamiltonian.

In the conventional approach based on equal-time quantization the Fock state expansion becomes quickly intractable because of the complexity of the vacuum. Furthermore, boosting such a wavefunction from the hadron's rest frame to a moving frame is as complex a problem as solving the bound state problem itself. The presence of the square root operator in the equal-time Hamiltonian approach presents severe mathematical difficulties.

Fortunately 'light-cone quantization' offers an elegant avenue of escape. It can be formulated independent of the Lorentz frame. The square root operator does not appear, and the vacuum structure is relatively simple. There is no spontaneous creation of massive fermions in the light-cone quantized vacuum.

In fact, there are many reasons to quantize relativistic field theories at fixed light-cone time. Dirac [1] showed, in 1949, that in this so called 'front form' of Hamiltonian dynamics a maximum number of Poincaré generators become independent of the interaction, including certain Lorentz boosts. In fact, unlike the traditional equal-time Hamiltonian formalism, quantization on a plane tangential to the light-cone, on the 'null plane', can be formulated without reference to a specific frame. One can construct an operator whose eigenvalues are the invariant masses of the composite physical particles. The eigenvectors describe bound states of arbitrary four-momentum and invariant mass, and allow the computation of scattering amplitudes and other dynamical quantities. In many field theories the vacuum state of the free Hamiltonian is also an eigenstate of the light-cone

Hamiltonian. The Fock expansion built on this vacuum state provides a complete relativistic many-particle basis for diagonalizing the full theory.

The main thrust of these lectures will be to discuss the complexities that are unique to this formulation of QCD, in varying degrees of detail. The goal is to present a self-consistent framework rather than trying to cover the subject exhaustively. A review all of the successes or applications will, however, not be undertaken.

One of the reasons is, that the subject was reviewed recently [2]. Another is that other lecturers in this school emphasize complementary aspects. Stan Brodsky shows how the knowledge of the the light-cone wavefunction has impact on hadronic physics and exclusive processes. Steve Pinsky demonstrates how the method of discretized light-cone quantization is constructive for analyzing supersymmetric string and M(atrix) theories. Last not least, Simon Dalley expands on the transverse-lattice calculations within the light-cone approach.

Comparatively little space will be devoted to canonical field theory, just so much as to plausibilize that a light-cone Hamiltonian exists. This so called 'naive Hamiltonian' will be derived and written down explicitly as a Fock-space operator in the light-cone gauge and disregarding zero modes. For historical and paedagogical reasons these notes will be rather outspoken for one space and one time dimension, mostly to show that periodic boundary conditions (discretized light-cone quantization) are helpful, indeed, for solving the bound-state problem in a relativistic theory. The attempt is made to be complementary to the review [2] and some new material on the Schwinger model is included.

The bulk of these notes deals with the many-body aspects of a gauge field theory in the real world of 3+1 dimensions. A hadron not only contains the valence quarks but also an infinite amount of gluons and sea-quarks. Progress often comes with new technologies. The presentation of the method of iterated resolvents therefore takes broad room. It allows to derive a well-defined effective interaction. Some thus far unpublished work is included, in particular more instructive examples. The presentation is separated into two parts. In the first considerations are essentially exact. In the second some approximations and simplifications are admitted and well marked in the text. One arrives at the effective interaction in the form of a tractable and solvable integral equation. Its solutions allow to construct explicitly the many-body amplitudes corresponding to see-quarks and gluons by comparatively simple quadratures, without the need of solving another bound-state problem. Explicit equations for that are given. Moreover, some new research work will be included in the section on renormalization.

What is not included in these notes, however, is a complete survey of the literature. Mostly for the reasons of space, it is refered to the some 469 items of [2]. I apologize with my colleagues whose work is not mentioned. But I will be careful to cite the work which I need for the present discussion and presentation. Some selected monographies which I found useful to consult are [3, 4, 5, 6, 7], some selected review articles or conference proceedings might be [8, 9, 10, 11].

2 Forms of Hamiltonian Dynamics

Dirac defines the Hamiltonian H of a closed system as that operator whose action on the state vector $\mid t \rangle$ has the same effect as taking the partial derivative with respect to time t, *i.e.*

$$H \mid t \rangle = i\frac{\partial}{\partial t} \mid t \rangle. \tag{1}$$

The concept of an Hamiltonian is applicable irrespective of whether one deals with the motion of a non-relativistic particle in classical mechanics or with a non-relativistic wave function in the Schrödinger equation, and it generalizes almost unchanged to a relativistic and covariant field theory.

In a covariant theory, the very notion of 'time' becomes, however, questionable since the time is only one component of four-dimensional space-time. But the concept of usual space and of usual time can be generalized. One can define 'space' as that hypersphere in four-space on which one chooses the initial conditions. The remaining fourth coordinate can be understood as 'time'.

More formally, one conveniently introduces generalized coordinates $\widetilde{x}^\nu$. Starting from a baseline parametrization of space-time like the instant form in Figure 1, one parametrizes space-time by a coordinate transformation $\widetilde{x}^\nu = \widetilde{x}^\nu(x^\mu)$. The metric tensors for the two parametrizations are then related by

$$\widetilde{g}_{\kappa\lambda} = \left(\frac{\partial x^\mu}{\partial \widetilde{x}^\kappa}\right) g_{\mu\nu} \left(\frac{\partial x^\nu}{\partial \widetilde{x}^\lambda}\right).$$

The physical content of the theory can not depend on such a re-parametrization.

But the raising and the lowering of Lorentz indices are then non-trivial operations. As an example consider the front form parametrization in Figure 1. Interpret $\widetilde{x}^3 = x^0 - x^3$ as the new space coordinate and denote it by $x^- = ct - z$. Then $\widetilde{x}^0 = x^0 + x^3$ must be interpreted as the new time coordinate denoted by $x^+ = ct + z$, or by the 'light-cone time' $\tau = t + z/c$. Of course, one also could exchange the two. Since the lowering operation is $x_\mu = g_{\mu\nu}x^\nu$, both $x_+ = \frac{1}{2}x^-$ are space, and $x_- = \frac{1}{2}x^+$ are time coordinates. The new space derivative is therefore $\partial_- = \frac{1}{2}\partial^+$, while $\partial_+ = \frac{1}{2}\partial^-$ is a time-derivative. The Lorentz indices '+' and '-' have a different physical meaning, depending on whether they occur up- or down-stairs. Co-variant and contra-variant vectors are different objects. The Hamiltonian is only one component of a four-vector P^μ, particularly its time-like component. Taking the partial time derivative of the state vector

$$P_+ \mid x^+ \rangle = i\frac{\partial}{\partial x^+} \mid x^+ \rangle,$$

defines then $P_+ = \frac{1}{2}P^-$ as the Hamiltonian in the transformed coordinates, in line with Eq.(1), and $P_- = \frac{1}{2}P^+$ as the longitudinal momentum.

Following Dirac [1] there are no more than three different parametrisations of space-time. They are illustrated in Figure 1, and cannot be mapped onto each

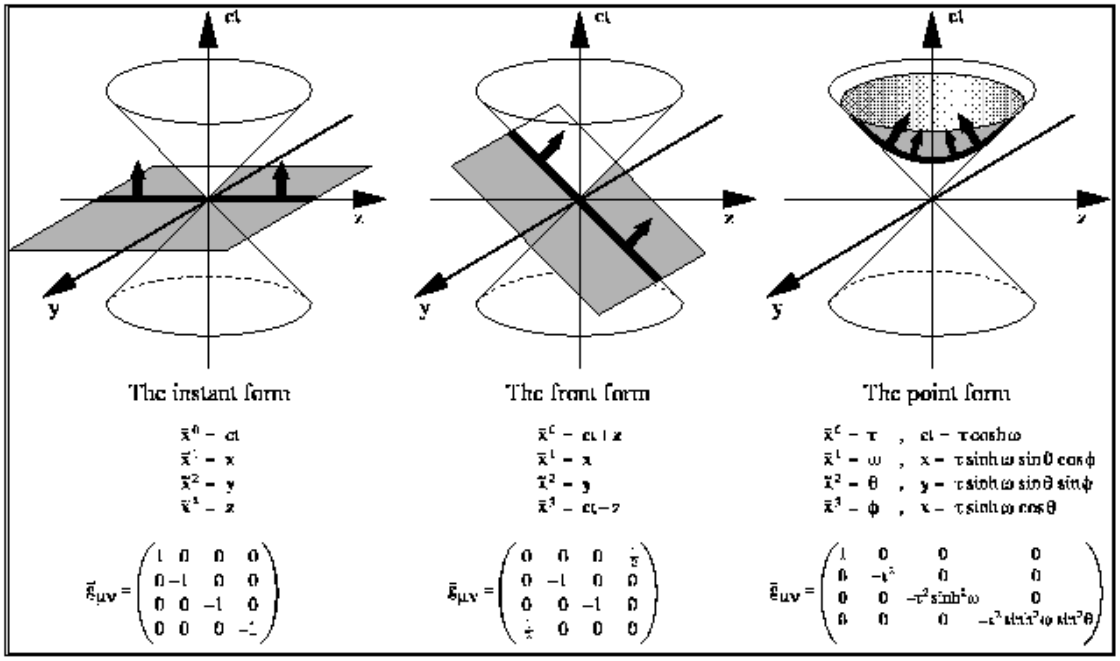

Figure 1: Dirac's three forms of Hamiltonian dynamics.

other by a Lorentz transform. They differ by the hypersphere on which the fields are initialized. They have thus different 'times' and different 'Hamiltonians'. Dirac [1] speaks of the three *forms of Hamiltonian dynamics*: The *instant form* is the familiar one, with its hypersphere given by $t = 0$. In the *front form* the hypersphere is a tangent plane to the light cone. In the *point form* the time-like coordinate is identified with the eigentime of a physical system and the hypersphere has a shape of a hyperboloid.

Which of the three forms should be prefered, is an ill-posed question, since all three forms must yield the same physical results. Comparatively little work has been done in the point form. The bulk of research on field theory implicitly uses the instant form. Although it is the conventional choice for quantizing field theory, it has many practical disadvantages. For example, given the wavefunctions of an n-electron atom at an initial time $t = 0$, $\psi_n(\vec{x}_i, t = 0)$, one can use the Hamiltonian H to evolve $\psi_n(\vec{x}_i, t)$ to later times t. However, an experiment which specifies the initial wave function would require the simultaneous measurement of the positions of all of the bounded electrons. In contrast, determining the initial wave function at fixed light-cone time $\tau = 0$ only requires an experiment which scatters one plane-wave laser beam, since the signal reaching each of the n electrons, along the light front, at the same light-cone time $\tau = t_i + z_i/c$.

Dirac's legacy had been forgotten and was re-invented several times. The front form approach carries therefore names as different as *Infinite-Momentum Frame*, *Null-Plane Quantization*, *Light-Cone Quantization*, or most recently *Light-Front*

Quantization. In the essence they are all the same. The infinite-momentum frame is a misnomer since the total momentum is finite and since the front form is *frame-independent* and covariant. Light-cone quantization is also unfortunate, since the inital data are set one a plane tangential to but not on the light cone, and since both equal-time or equal light-cone-time quantization stand both for the same quantization, for a quantum as opposed to a classical theory. We propose to stay with Dirac's different 'forms of Hamiltonians'.

2.1 The canonical Hamiltonian for gauge theory

The prototype of a field theory is Faraday's and Maxwell's electrodynamics. Every field theory has its own canonical Hamiltonian and is governed by the action density. The Lagrangian is the subject of the canonical calculus of variation, given in many text books [4]. Its essentials shall be recalled briefly.

The Lagrangian, in general, is a function of a finite number of fields $\phi_r(x)$ and their first space-time derivatives $\partial_\mu\phi_r(x)$, thus $\mathcal{L} = \mathcal{L}\left[\phi_r, \partial_\mu\phi_r\right]$. Independent variation of $\mathcal{L}$ with respect to ϕ_r and $\partial_\mu\phi_r$ results in the equations of motion,

$$\partial_\kappa \pi_r^\kappa - \delta\mathcal{L}/\delta\phi_r = 0 \ , \quad \text{with} \quad \pi_r^\kappa[\phi] \equiv \frac{\delta\mathcal{L}}{\delta\left(\partial_\kappa\phi_r\right)},$$

canonically refered to as the Euler equations. The canonical formalism is particularly suited for discussing the symmetries of a field theory. Every continuous symmetry of the Lagrangian is associated with a vanishing four-divergence of a current and a conserved charge. Since $\mathcal{L}$ does not explicitely depend on the coordinates, every field theory in 3+1 dimensions has ten conserved four-currents. The four-divergences of the energy-momentum tensor $T^{\lambda\nu}$ and of the boost-angular--momentum stress tensor $J^{\lambda,\mu\nu}$ vanish,

$$\partial_\lambda T^{\lambda\nu} = 0, \quad \partial_\lambda J^{\lambda,\mu\nu} = 0.$$

As a consequence the Lorentz group has ten 'conserved charges', the 4 components total momentum P^ν and the 6 components of boost-angular momentum $M^{\mu\nu}$,

$$P^\nu = \int_\Omega d\omega_0 T^{0\nu} \ , \quad \text{and} \qquad M^{\mu\nu} = \int_\Omega d\omega_0 J^{0,\mu\nu}. \tag{2}$$

With the totally antisymmetric tensor in four dimensions $\epsilon_{\lambda\mu\nu\rho}$ ($\epsilon_{0123} = 1$), the three-dimensional surface elements of a hypersphere are $d\omega_\lambda = \epsilon_{\lambda\mu\nu\rho}dx^\mu dx^\nu dx^\rho/3!$. A finite volume is thus $\Omega = \int d\omega_0 = \int dx^1dx^2dx^3$, and correspondingly in the front form $d\omega_+ = \int dx_+ d^2x_\perp$. The time-like components of P_μ is the Hamiltonian, *i.e.* P_0 for the instant form and P_+ for the front form. The transition from instant to front form is thus simple: substitute '0' by '+'.

Working out the canonical procedure for QED with its Lagrangian,

$$\mathcal{L} = -\frac{1}{4}F^{\mu\nu}F_{\mu\nu} + \frac{1}{2}\left[\overline{\Psi}\left(i\gamma^\mu D_\mu - m\right)\Psi + \text{ h.c. }\right], \tag{3}$$

where $F^{\mu\nu}$ is the electro-magnetic field tensor and D_μ the covariant derivative,

$$F^{\mu\nu} = \partial^\mu A^\nu - \partial^\nu A^\mu, \qquad D_\mu = \partial_\mu - igA_\mu,$$

one ends up with a manifestly gauge-invariant total momentum,

$$\begin{aligned} P_\nu &= \int_\Omega d\omega_0 \left(F^{0\kappa}F_{\kappa\nu} + \frac{1}{4}g^0_\nu F^{\kappa\lambda}F_{\kappa\lambda} + \frac{1}{2}\Big[i\overline{\Psi}\gamma^0 D_\nu \Psi + \text{ h.c.}\Big]\right), \\ P_\nu &= \int_\Omega d\omega_+ \left(F^{+\kappa}F_{\kappa\nu} + \frac{1}{4}g^+_\nu F^{\kappa\lambda}F_{\kappa\lambda} + \frac{1}{2}\Big[i\overline{\Psi}\gamma^+ D_\nu \Psi + \text{ h.c.}\Big]\right), \end{aligned}$$

in both the instant and the front form, respectively. The boost angular momenta will not be used explicitly.

The gauge invariant Lagrangian density for QCD is

$$\begin{aligned} \mathcal{L} &= -\frac{1}{2}\mathrm{Tr}(\mathbf{F}^{\mu\nu}\mathbf{F}_{\mu\nu}) + \frac{1}{2}[\overline{\Psi}(i\gamma^\mu \mathbf{D}_\mu - \mathbf{m})\Psi + \text{ h.c.}], \\ &= -\frac{1}{4}F^{\mu\nu}_a F^a_{\mu\nu} + \frac{1}{2}[\overline{\Psi}(i\gamma^\mu \mathbf{D}_\mu - \mathbf{m})\Psi + \text{ h.c.}], \end{aligned}$$

The color-electro-magnetic fields and the covariant derivative are now

$$\begin{aligned} \mathbf{F}^{\mu\nu} \equiv \partial^\mu \mathbf{A}^\nu - \partial^\nu \mathbf{A}^\mu + ig[\mathbf{A}^\mu, \mathbf{A}^\nu] &= \mathbf{T}^a \left(\partial^\mu A^\nu_a - \partial^\nu A^\mu_a - g f^{ars} A^\mu_r A^\nu_s\right), \\ \mathbf{D}^\mu_{cc'} = \delta_{cc'}\partial^\mu + ig\mathbf{A}^\mu_{cc'} &= \delta_{cc'}\partial^\mu + igT^a_{cc'}A^\mu_a. \end{aligned}$$

As compared to QED, each local gauge field $A^\mu(x)$ is replaced by the 3×3 matrix $\mathbf{A}^\mu(x)$. All such matrices can be parametrized $\mathbf{A}^\mu \equiv T^a_{cc'}A^\mu_a$. More generally for SU(N), the vector potentials $\mathbf{A}^\mu$ are hermitian and traceless $N\times N$ matrices. The color index c (or c') runs now from 1 to n_c, and correspondingly the gluon index a (or r, s, t) from 1 to $n_c^2 - 1$. No distinction will be made between raising or lowering them. In order to make sense of expressions like $\overline{\Psi}\mathbf{A}^\mu\Psi$ the quark fields $\Psi_{c,\alpha}(x)$ must carry a color index c. They, as well as the Dirac indices, are usually suppressed. The color matrices $T^a_{cc'}$ obey

$$\Big[T^r, T^s\Big]_{cc'} = if^{rsa}T^a_{cc'} \qquad \text{and} \qquad \mathrm{Tr}\ (T^r T^s) = \frac{1}{2}\delta^s_r. \tag{4}$$

For SU(2) the color matrices are $T^a = \frac{1}{2}\sigma^a$, with σ^a being the Pauli matrices. The structure constants f^{rst} are therefore the totally antisymmetric tensor ϵ_{rst}. For SU(3), $T^a = \frac{1}{2}\lambda^a$ with the Gell-Mann matrices λ^a, with the corresponding structure constants tabulated in the literature [6]. Everything proceeds in analogy with QED. The energy-momentum vector,

$$\begin{aligned} P_\nu &= \int_\Omega d\omega_0 \left(F^{0\kappa}_a F^a_{\kappa\nu} + \frac{1}{4}g^0_\nu F^{\kappa\lambda}_a F^a_{\kappa\lambda} + \frac{1}{2}\Big[i\overline{\Psi}\gamma^0 T^a D^a_\nu \Psi + \text{ h.c.}\Big]\right), \\ P_\nu &= \int_\Omega d\omega_+ \left(F^{+\kappa}_a F^a_{\kappa\nu} + \frac{1}{4}g^+_\nu F^{\kappa\lambda}_a F^a_{\kappa\lambda} + \frac{1}{2}\Big[i\overline{\Psi}\gamma^+ T^a D^a_\nu \Psi + \text{ h.c.}\Big]\right), \end{aligned} \tag{5}$$

is manifestly gauge-invariant both in the instant and the front form.

2.2 The Poincaré symmetries in the front form

The ten constants of motion P^μ and $M^{\mu\nu}$ are observables with real eigenvalues. It is advantageous to construct representations in which the constants of motion are diagonal. But one cannot diagonalize all ten constants of motion simultaneously because they do not commute. The algebra of the four-energy-momentum $P^\mu = p^\mu$ and four-angular-momentum $M^{\mu\nu} = x^\mu p^\nu - x^\nu p^\mu$ for free particles with the basic commutator $\frac{1}{i\hbar}[x^\mu, p_\nu] = \delta^\mu_\nu$ is

$$\begin{aligned} \frac{1}{i\hbar}\,[P^\rho, M^{\mu\nu}] &= g^{\rho\mu}P^\nu - g^{\rho\nu}P^\mu\ , \quad \frac{1}{i\hbar}\,[P^\rho, P^\mu] = 0\ , \\ \text{and} \quad \frac{1}{i\hbar}\,[M^{\rho\sigma}, M^{\mu\nu}] &= g^{\rho\nu}M^{\sigma\mu} + g^{\sigma\mu}M^{\rho\nu} - g^{\rho\mu}M^{\sigma\nu} - g^{\sigma\nu}M^{\rho\mu}. \end{aligned}$$

It is postulated that the generalized momentum operators satisfy the same commutator relations as a single particle. They form thus a group, the Poincaré group.

It is convenient to discuss the structure of the Poincaré group in terms of the Pauli-Lubansky vector $V^\kappa \equiv \epsilon^{\kappa\lambda\mu\nu}P_\lambda M_{\mu\nu}$. V is orthogonal to the generalized momenta, $P_\mu V^\mu = 0$. The two group invariants are the operator for the invariant mass-squared $M^2 = P^\mu P_\mu$ and the operator for intrinsic spin-squared $V^2 = V^\mu V_\mu$. They are Lorentz scalars and commute with all generators P^μ and $M^{\mu\nu}$, as well as with all V^μ. A convenient choice of six mutually commuting operators is: The invariant mass squared $M^2 = P^\mu P_\mu$, the three space-like momenta P^+ and $\vec{P}_\perp$, the total spin squared $S^2 = V^\mu V_\mu$, and one component of V, say $V^+ \equiv S_z$.

Inspecting the definition of boost-angular momentum $M_{\mu\nu}$ in Eq.(2) one identifies which components are dependent on the interaction and which are not. Dirac [1] calls them complicated and simple, or dynamic and kinematic, or Hamiltonians and Momenta, respectively. In the instant form, the three components of the boost vector $K_i = M_{i0}$ are dynamic, and the three components of angular momentum $J_i = \epsilon_{ijk}M_{jk}$ are kinematic. As noted already by Dirac, the front form is special in having four kinematic components of $M_{\mu\nu}$ ($M_{+-}, M_{12}, M_{1-}, M_{2-}$) and only two dynamic ones (M_{+1} and M_{+2}). In the front form one deals thus with seven mutually commuting operators

$$(M_{+-}, M_{12}, M_{1-}, M_{2-}), \quad \text{and all } P^\mu,$$

instead of the six in the instant form. These symmetries imply the very important aspect of the front form that both the Hamiltonian and all amplitudes obtained in light-cone perturbation theory are manifestly invariant under a large class of Lorentz transformations:

$$\begin{array}{lll} p^+ \to C_\parallel\, p^+\,, & \vec{p}_\perp \to \vec{p}_\perp\,, & p^- \to C_\parallel^{-1} p^-\,, \\ p^+ \to p^+\,, & \vec{p}_\perp \to \vec{p}_\perp + p^+\vec{C}_\perp\,, & p^- \to p^- + 2\vec{p}_\perp\cdot\vec{C}_\perp + p^+\vec{C}_\perp^{\,2}\,, \\ p^+ \to p^+\,, & \vec{p}_\perp^{\,2} \to \vec{p}_\perp^{\,2}\,, & \end{array}$$

i.e. for parallel boosts, transverse boosts, and rotations, respectively. All of these hold for every single particle momentum p^μ, and for any set of dimensionless c-numbers $C_\parallel$ and $\vec{C}_\perp$.

2.3 The light-cone Hamiltonian operator

The four-vector of energy-momentum for gauge theory in Eq.(5) contains time-derivatives and other constraint field components. They will be eliminated in this section using the equations of motion with the goal to express P^ν in terms of the free fields and to isolate the dependence on the coupling constant.

The color-Maxwell equations are four equations for determining the four functions A^μ_a. One of the equations of motion is identically fullfilled by choosing the light-cone gauge $A^+_a = 0$. Two of the equations give expressions the time derivatives of the two transversal components $\vec{A}^a_\perp$. The fourth is the Gauss' law in the front form, $\partial_\mu F^{\mu+}_a = g J^+_a$, or explicitly

$$-\partial^+\partial_- A^-_a - \partial^+\partial_i A^i_{\perp a} = g J^+_a. \tag{6}$$

It contains only space-derivatives and is a constrained equation for the components of A^μ_a. For the free case ($g = 0$), A^μ_a reduces to $\widetilde{A}^\mu_a$ and therefore to

$$\widetilde{A}^\mu_a = \left(\widetilde{A}^+_a, \vec{A}_{\perp a}, \widetilde{A}^-_a\right) = \left(0, \vec{A}_{\perp a}, -\frac{1}{\partial_-}\left[\partial_i A^i_{\perp a}\right]\right).$$

As a consequence, $\widetilde{A}^\mu_a$ is purely transverse. The formal inversion of Eq.(6) is therefore

$$A^-_a = \widetilde{A}^-_a + \frac{g}{(i\partial_-)^2} J^+_a, \tag{7}$$

which must be substituted everywhere. The inverse space derivatives $(i\partial^+)^{-1}$ and $(i\partial^+)^{-2}$, used here and below, are actually Green's functions. Since they depend only on x^-, they are comparatively simple.

The color-Dirac equations $(i\gamma^\mu \mathbf{D}_\mu - \mathbf{m})\Psi = 0$ can be used to express the time derivatives $\partial_+\Psi$ as function of the other fields. After multiplication with γ^0 one gets first

$$(i\gamma^0\gamma^+ T^a D^a_+ + i\gamma^0\gamma^- T^a D^a_- + i\alpha^i_\perp T^a D^a_{\perp i})\Psi = m\beta\Psi,$$

with the usual Dirac matrices $\beta = \gamma^0$ and $\alpha^k = \gamma^0\gamma^k$. In order to isolate the time derivative one introduces the projectors $\Lambda_\pm$ and projected spinors $\Psi_\pm$ by

$$\Lambda_\pm = \frac{1}{2}(1 \pm \alpha^3) \qquad \text{and} \qquad \Psi_\pm = \Lambda_\pm \Psi\ .$$

Multiplying the color-Dirac equation once with Λ_+ and once with Λ_- gives

$$\begin{aligned} 2i\partial_+\Psi_+ &= \left(m\beta - i\alpha^i_\perp T^a D^a_{\perp i}\right)\Psi_- + 2gA^a_+ T^a \Psi_+, \\ \text{and}\quad 2i\partial_-\Psi_- &= \left(m\beta - i\alpha^i_\perp T^a D^a_{\perp i}\right)\Psi_+ + 2gA^a_- T^a \Psi_-, \end{aligned} \tag{8}$$

a coupled set of spinor equations. The first of them contains a time derivative. The second contains a space derivative and is a constraint equation. The component

$$\Psi_- = \frac{1}{2i\partial_-}\left(m\beta - i\alpha^i_\perp T^a D^a_{\perp i}\right)\Psi_+ \tag{9}$$

must therefore be substituted everywhere. The time derivative becomes then

$$2i\partial_+\Psi_+ = 2gA^a_+T^a\Psi_+ + \left(m\beta - i\alpha^j_\perp T^a D^a_{\perp j}\right)\frac{1}{2i\partial_-}\left(m\beta - i\alpha^i_\perp T^a D^a_{\perp i}\right)\Psi_+ .$$

In analogy to the color-Maxwell case one defines free spinors by

$$\widetilde{\Psi} = \Psi_+ + \left(m\beta - i\alpha^i_\perp \partial_{\perp i}\right)\frac{1}{2i\partial_-}\Psi_+ .$$

Contrary to the full spinor, $\widetilde{\Psi}$ is independent of the interaction.

Inserting the above expressions into Eq.(5), the space-like components of P^ν become

$$P_k = \int dx_+ d^2x_\perp \Big(\overline{\widetilde{\Psi}}\ \gamma^+ i\partial_k\widetilde{\Psi} + \widetilde{A}^\mu_a\ \partial^+\partial_k\widetilde{A}^a_\mu\Big)\ , \qquad \text{for } k = 1, 2, -. \tag{10}$$

Inserting them into P_+ gives rather lengthy expressions, which are conveniently written as a sum of five terms

$$P_+ = T + V + W_1 + W_2 + W_3. \tag{11}$$

Only the first term survives the limit $g \to 0$, and therefore is called the free part of the Hamiltonian, or its 'kinetic energy'

$$T = \frac{1}{2}\int dx_+ d^2x_\perp \Big(\overline{\widetilde{\Psi}}\gamma^+\frac{m^2 + (i\nabla_\perp)^2}{i\partial^+}\widetilde{\Psi} + \widetilde{A}^\mu_a (i\nabla_\perp)^2\widetilde{A}^a_\mu\Big).$$

The vertex interaction

$$V = g\int dx_+ d^2x_\perp\ \widetilde{J}^\mu_a\widetilde{A}^a_\mu, \qquad \text{with} \quad \widetilde{J}^\nu_a(x) = \overline{\widetilde{\Psi}}\gamma^\nu T^a\widetilde{\Psi} + f^{abc}\partial^\mu\widetilde{A}^\nu_b\widetilde{A}^c_\nu, \tag{12}$$

is linear in the coupling constant and is the light-cone analogue of the conventional $J_\mu A^\mu$-structures in the instant form. Note that the current $\widetilde{J}^\mu_a$ has contributions from both quarks and gluons. The four-point gluon interaction

$$W_1 = \frac{g^2}{4}\int dx_+ d^2x_\perp\ \widetilde{B}^{\mu\nu}_a\widetilde{B}^a_{\mu\nu}, \qquad \text{with} \quad B^{\mu\nu}_a = f^{abc}\widetilde{A}^\mu_b\widetilde{A}^\nu_c,$$

describes the four-point gluon-vertices which is quadratic in g. The remainders are the 'instantaneous interactions'. They are characterized by the inverse derivatives. The instantaneous gluon interaction arises from the Gauss equation,

$$W_2 = \frac{g^2}{2}\int dx_+ d^2x_\perp\ \widetilde{J}^+_a\frac{1}{(i\partial^+)^2}\widetilde{J}^+_a,$$

and is the light-cone analogue of the Coulomb energy. The instantaneous fermion interaction originates from the light-cone specific decomposition of Dirac's equation

$$W_3 = \frac{g^2}{2}\int dx_+ d^2x_\perp\ \overline{\widetilde{\Psi}}\gamma^\mu T^a\widetilde{A}^a_\mu\ \frac{\gamma^+}{i\partial^+}\left(\gamma^\nu T^b\widetilde{A}^b_\nu\widetilde{\Psi}\right).$$

It has no analogue in the instant form.

Most remarkable, however, is that the relativistic Hamiltonian is additive in the 'kinetic' and the 'potential' energy, very much like a non-relativistic Hamiltonian $H = T + U$. In this respect the front form is distinctly different from the conventional instant form.

2.4 The free field solutions

The free solutions of the Dirac and the Maxwell equations are in the front form

$$\begin{aligned}
\widetilde{\Psi}_{\alpha cf}(x) &= \sum_\lambda \int \frac{dp^+ d^2p_\perp}{\sqrt{2p^+(2\pi)^3}} \left(b(q) u_\alpha(p,\lambda) e^{-ipx} + d^\dagger(q) v_\alpha(p,\lambda) e^{+ipx} \right), \\
\widetilde{A}^a_\mu(x) &= \sum_\lambda \int \frac{dp^+ d^2p_\perp}{\sqrt{2p^+(2\pi)^3}} \left(a(q) \epsilon_\mu(p,\lambda) e^{-ipx} + a^\dagger(q) \epsilon^\star_\mu(p,\lambda) e^{+ipx} \right).
\end{aligned}$$

The properties of the Dirac spinors u_α and v_α, and of the polarization vectors ϵ_μ, are given for example in [2]. The single particle state are specified by the quantum numbers $q = (p^+,\, p_{\perp x},\, p_{\perp y},\, \lambda,\, c,\, f)$. Their creation and destruction operators are subject to the usual relations

$$\left[a(q), a^\dagger(q')\right] = \left\{b(q), b^\dagger(q')\right\} = \left\{d(q),\ d^\dagger(q')\right\} = \delta(p^+ - p^{+\prime})\delta^{(2)}(\vec{p}_\perp - \vec{p}'_\perp)\delta^{\lambda'}_\lambda \delta^{c'}_c \delta^{f'}_f,$$

which carry the operator structure of the theory. When inserting the free fields into P_μ one can integrate out the dependence on x^μ, producing essentially Dirac delta-functions in the single particle momenta, which reflect momentum conservation:

$$\int \frac{dx_+}{2\pi} e^{ix_+\left(\sum_j p_j^+\right)} = \delta\Big(\sum_j p_j^+\Big), \qquad \int \frac{d^2x_\perp}{(2\pi)^2} e^{-i\vec{x}_\perp\left(\sum_j \vec{p}_{\perp j}\right)} = \delta^{(2)}\Big(\sum_j \vec{p}_{\perp j}\Big).$$

In detail this can be quite laborious, as shown by the example with the fermionic contribution to the vertex interaction

$$\begin{aligned}
V_f &= g \int dx_+ d^2x_\perp \ \overline{\widetilde{\Psi}}(x) \gamma^\mu T^a \widetilde{\Psi}(x) \widetilde{A}^a_\mu(x) \Big|_{x^+=0} \\
&= \frac{g}{\sqrt{(2\pi)^3}} \sum_{\lambda_1,\lambda_2,\lambda_3} \sum_{c_1,c_2,a_3} \int \frac{dp_1^+ d^2p_{\perp 1}}{\sqrt{2p_1^+}} \int \frac{dp_2^+ d^2p_{\perp 2}}{\sqrt{2p_2^+}} \int \frac{dp_3^+ d^2p_{\perp 3}}{\sqrt{2p_3^+}} \\
&\times \int \frac{dx_+ d^2x_\perp}{(2\pi)^3} \Big[\Big(b^\dagger(q_1) \overline{u}_\alpha(p_1,\lambda_1) e^{+ip_1x} + d(q_1) \overline{v}_\alpha(p_1,\lambda_1) e^{-ip_1x} \Big) T^{a_3}_{c_1,c_2} \\
&\times \qquad \gamma^\mu_{\alpha\beta} \left(d^\dagger(q_2) v_\beta(p_2,\lambda_2) e^{+ip_2x} + b(q_2) u_\beta(p_2,\lambda_2) e^{-ip_2x} \right) \Big] \\
&\times \qquad\quad \left(a^\dagger(q_3) \epsilon^\star_\mu(p_3,\lambda_3) e^{+ip_3x} + a(q_3) \epsilon_\mu(p_3,\lambda_3) e^{-ip_3x} \right).
\end{aligned}$$

Note that the sum of these single particle momenta is essentially the sum of the particle momenta minus the sum of the hole momenta. Consequently, if a particular

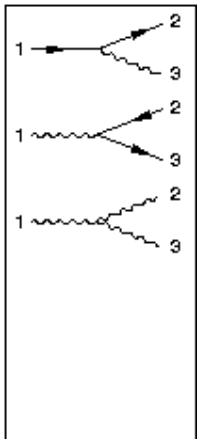

$$
\begin{aligned}
V_1 &+ \frac{\Delta_V}{\sqrt{k_1^+ k_2^+ k_3^+}}\ (\bar{u}_1 \not{\epsilon}_3 T^{a_3} u_2) \\
V_3 &+ \frac{\Delta_V}{\sqrt{k_1^+ k_2^+ k_3^+}}\ (\bar{v}_2 \not{\epsilon}_1^\star T^{a_1} u_3) \\
V_4 = &\frac{iC^{a_1}_{a_2 a_3}\,\Delta_V}{\sqrt{k_1^+ k_2^+ k_3^+}}\ (\epsilon_1^\star k_3)\ (\epsilon_2 \epsilon_3) \\
&+ \frac{iC^{a_1}_{a_2 a_3}\,\Delta_V}{\sqrt{k_1^+ k_2^+ k_3^+}}\ (\epsilon_3 k_1)\ (\epsilon_1^\star \epsilon_2) \\
&+ \frac{iC^{a_1}_{a_2 a_3}\,\Delta_V}{\sqrt{k_1^+ k_2^+ k_3^+}}\ (\epsilon_3 k_2)\ (\epsilon_1^\star \epsilon_2)
\end{aligned}
$$

Table 1: *The vertex interaction in terms of Dirac spinors. The matrix elements V_n are displayed on the right, the corresponding (energy) graphs on the left. All matrix elements are proportional to $\Delta_V = \widehat{g}\delta(k_1^+|k_2^+ + _3)\delta^{(2)}(\vec{k}_{\perp,1}|\vec{k}_{\perp,2} + \vec{k}_{\perp,3})$, with $\widehat{g} = g/\sqrt{2(2\pi)^3}$. For the periodic boundary conditions one uses $\widehat{g} = g/\sqrt{\Omega}$.*

term has only creation or only destruction operators as in

$$b^\dagger(q_1) d^\dagger(q_2) a^\dagger(q_3)\ \delta\Big(p_1^+ + p_2^+ + p_3^+\Big) \simeq 0,$$

its contribution vanishes since the light-cone longitudinal momenta p^+ are all positive and can not add to zero. As a consequence, all energy diagrams which generate the vacuum fluctuations in the usual formulation of quantum field theory are absent in the front form.

2.5 The Hamiltonian as a Fock-space operator

The *kinetic energy* T becomes a sum of 3 diagonal operators

$$
\begin{aligned}
T &= \int dk_- d^2\vec{k}_\perp \sum_{\lambda,c,f} \Big(\frac{m^2 + \vec{k}_\perp^2}{k_-}\Big)_q \Big(b_q^\dagger b_q + d_q^\dagger d_q + a_q^\dagger a_q\Big) \\
&\equiv \sum_q \Big(\frac{m^2 + \vec{k}_\perp^2}{k_-}\Big)_q \Big(b_q^\dagger b_q + d_q^\dagger d_q + a_q^\dagger a_q\Big)\,.
\end{aligned}
$$

Here and in the sequel it is convenient to abbreviate the integration and summation over the single particle coordinates by the symbol $\sum$ to replace for instance $b(q)$ with b_q.

The *vertex interaction* V becomes a sum of 4 operators

$$V = V_1 + V_2 + V_3 + V_4$$

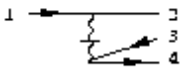	F_1	$= +\dfrac{2\Delta}{\sqrt{k_1^+k_2^+k_3^+k_4^+}}\dfrac{(\bar{u}_1 T^a\gamma^+ u_2)\ (\bar{v}_3\gamma^+ T^a u_4)}{(k_1^+-k_2^+)^2}$
	$F_{3,1}$	$= +\dfrac{\Delta}{\sqrt{k_1^+k_2^+k_3^+k_4^+}}\dfrac{(\bar{u}_1 T^{a_4}\not{\epsilon}_4\gamma^+\not{\epsilon}_3 T^{a_2} u_2)}{(k_1^+-k_4^+)}$
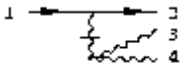	$F_{3,2}$	$= -\dfrac{2k_3^+\Delta}{\sqrt{k_1^+k_2^+k_3^+k_4^+}}\dfrac{(\bar{u}_1 T^a\gamma^+ u_2)\ (\epsilon_3 i C^a\epsilon_4)}{(k_1^+-k_2^+)^2}$
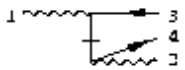	$F_{5,1}$	$= +\dfrac{\Delta}{\sqrt{k_1^+k_2^+k_3^+k_4^+}}\dfrac{(\bar{v}_3 T^{a_1}\not{\epsilon}_1^\star\gamma^+\not{\epsilon}_2 T^{a_2} u_4)}{(k_1^+-k_3^+)}$
	$F_{5,2}$	$= -\dfrac{\Delta}{\sqrt{k_1^+k_2^+k_3^+k_4^+}}\dfrac{(\bar{v}_3 T^{a_2}\not{\epsilon}_2\gamma^+\not{\epsilon}_1^\star T^{a_1} u_4)}{(k_1^+-k_4^+)}$
	$F_{5,3}$	$= +\dfrac{2(k_1^++k_2^+)\Delta}{\sqrt{k_1^+k_2^+k_3^+k_4^+}}\dfrac{(\bar{v}_3 T^a\gamma^+ u_4)\ (\epsilon_1^\star i C^a\epsilon_2)}{(k_1^+-k_2^+)^2}$
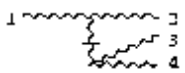	$F_{6,1}$	$= +\dfrac{2k_3^+(k_1^++k_2^+)\Delta}{\sqrt{k_1^+k_2^+k_3^+k_4^+}}\ \dfrac{(\epsilon_1^\star C^a\epsilon_2)\ (\epsilon_3 C^a\epsilon_4)}{(k_1^+-k_2^+)^2}$
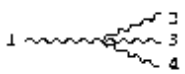	$F_{6,2}$	$= +\dfrac{2\Delta}{\sqrt{k_1^+k_2^+k_3^+k_4^+}}\ (\epsilon_1^\star\epsilon_3)\ (\epsilon_2\epsilon_4)\ C^a_{a_1a_2}C^a_{a_3a_4}$

Table 2: *The fork interaction in terms of Dirac spinors. The matrix elements $F_{n,j}$ are displayed on the right, the corresponding (energy) graphs on the left. All matrix elements are proportional to $\Delta = \widetilde{g}^2\delta(k_1^+|k_2^+ + k_3^+ + k_4^+)\delta^{(2)}(\vec{k}_{\perp,1}|\vec{k}_{\perp,2} + \vec{k}_{\perp,3} + \vec{k}_{\perp,4})$, with $\widehat{g} = g/\sqrt{2(2\pi)^3}$. For the periodic boundary conditions one uses $\widehat{g} = g/\sqrt{\Omega}$.*

$$
\begin{aligned}
= \quad & \sum_{1,2,3}\Big[b_1^\dagger b_2 a_3\, V_1(1;2,3) + \text{h.c.}\Big] + \sum_{1,2,3}\Big[d_1^\dagger d_2 a_3\, V_2(1;2,3) + \text{h.c.}\Big] + \\
+ \quad & \sum_{1,2,3}\Big[a_1^\dagger d_2 b_3\, V_3(1;2,3) + \text{h.c.}\Big] + \sum_{1,2,3}\Big[a_1^\dagger a_2 a_3\, V_4(1;2,3) + \text{h.c.}\Big]\ .
\end{aligned}
$$

It connects Fock states whose particle number differs by 1. The *matrix elements* $V_n(1;2,3) = V_n(q_1;q_2,q_3)$ are simple functions of the three single-particle states q_i, which are given in Table 1.

The four-point interactions are broken up conveniently into fork and seagull interactions, F and S, depending on whether they have an odd or an even number of creation operators, thus

$$P_+ = T + V + F + S.$$

The *fork interaction* F becomes then a sum of 6 operators,

$$F \quad = \quad F_1 + F_2 + F_3 + F_4 + F_5 + F_6$$

$$
\begin{aligned}
&= \sum_{1,2,3,4} \Big[b_1^\dagger b_2 d_3 b_4 \, F_1(1;2,3,4) + \text{h.c.}\Big] + \Big[d_1^\dagger d_2 b_3 d_4 \, F_2(1;2,3,4) + \text{h.c.}\Big] \\
&+ \sum_{1,2,3,4} \Big[b_1^\dagger b_2 a_3 a_4 \, F_3(1;2,3,4) + \text{h.c.}\Big] + \Big[d_1^\dagger d_2 a_3 a_4 \, F_4(1;2,3,4) + \text{h.c.}\Big] \\
&+ \sum_{1,2,3,4} \Big[a_1^\dagger a_2 d_3 b_4 \, F_5(1;2,3,4) + \text{h.c.}\Big] + \Big[a_1^\dagger a_2 a_3 a_4 \, F_6(1;2,3,4) + \text{h.c.}\Big] \,. \quad (13)
\end{aligned}
$$

It changes the particle number by 2. The matrix elements are given in Table 2.

The *seagull interaction* S, finally, becomes a sum of 7 operators

$$
\begin{aligned}
S &= S_1 + S_2 + S_3 + S_4 + S_5 + S_6 + S_7 \\
&= \sum_{1,2,3,4} b_1^\dagger b_2^\dagger b_3 b_4 \, S_1(1,2;3,4) + \sum_{1,2,3,4} d_1^\dagger d_2^\dagger d_3 d_4 \, S_2(1,2;3,4) \\
&+ \sum_{1,2,3,4} b_1^\dagger d_2^\dagger b_3 d_4 \, S_3(1,2;3,4) + \sum_{1,2,3,4} b_1^\dagger a_2^\dagger b_3 a_4 \, S_4(1,2;3,4) \\
&+ \sum_{1,2,3,4} d_1^\dagger a_2^\dagger d_3 a_4 \, S_5(1,2;3,4) + \sum_{1,2,3,4} (b_1^\dagger d_2^\dagger a_3 a_4 \, S_6(1,2;3,4) + \text{h.c.}) \\
&+ \sum_{1,2,3,4} a_1^\dagger a_2^\dagger a_3 a_4 \, S_7(1,2;3,4).
\end{aligned}
$$

Its matrix elements are given in Table 3. It can act only between Fock states with the same particle number.

The above results are are quite generally applicable: They hold for arbitrary non-abelian gauge theory $SU(N)$. They hold for abelian gauge theory (QED), formally by replacing the color-matrices $T^a_{c,c'}$ with the unit matrix and by setting to zero the structure constants f^{abc}, thus $B^{\mu\nu} = 0$ and $\chi^\mu = 0$. They hold for 1 time dimension and arbitrary $d+1$ space dimensions, with $i = 1, \ldots, d$. All what has to be adjusted is the volume integral $\int dx_+ dx_{\perp,1} \ldots dx_{\perp,d}$.

3 The hadronic bound-state problem

One has to find a language in which one can represent hadrons in terms of relativistic confined quarks and gluons. As reviewed in [12], the Bethe-Salpeter formalism has been the central method for analyzing hydrogenic atoms in QED and provides a completely covariant procedure for obtaining bound state solutions. However, calculations using this method are extremely complex and appear to be intractable much beyond the ladder approximation. It also appears impractical to extend this method to systems with more than a few constituent particles.

An intuitive approach for solving relativistic bound-state problems would be to solve the instant form Hamiltonian eigenvalue problem

$$H \, |\Psi\rangle = \sqrt{M^2 + \vec{P}^{\,2}} \, |\Psi\rangle$$

for the hadron's mass and wave function. Here, one imagines that $|\Psi\rangle$ is an expansion in multi-particle occupation number Fock states, and that the operators H

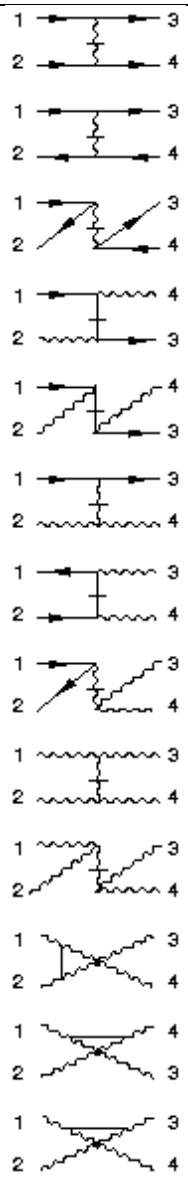

$$
\begin{aligned}
S_1 &= -\frac{\Delta}{\sqrt{k_1^+k_2^+k_3^+k_4^+}}\frac{(\bar u_1 T^a\gamma^+ u_3)\ (\bar u_2\gamma^+ T^a u_4)}{(k_1^+-k_3^+)^2}\\
S_{3,1} &= +\frac{2\Delta}{\sqrt{k_1^+k_2^+k_3^+k_4^+}}\frac{(\bar u_1 T^a\gamma^+ u_3)\ (\bar v_2\gamma^+ T^a v_4)}{(k_1^+-k_3^+)^2}\\
S_{3,2} &= -\frac{2\Delta}{\sqrt{k_1^+k_2^+k_3^+k_4^+}}\frac{(\bar v_2 T^a\gamma^+ u_1)\ (\bar v_4\gamma^+ T^a u_3)}{(k_1^++k_2^+)^2}\\
S_{4,1} &= +\frac{\Delta}{\sqrt{k_1^+k_2^+k_3^+k_4^+}}\frac{(\bar u_1 T^{a_4}\not\epsilon_4\gamma^+\not\epsilon_2^\star T^{a_2} u_3)}{(k_1^+-k_4^+)}\\
S_{4,2} &= +\frac{\Delta}{\sqrt{k_1^+k_2^+k_3^+k_4^+}}\frac{(\bar u_1 T^{a_2}\not\epsilon_2^\star\gamma^+\not\epsilon_4 T^{a_4} u_3)}{(k_1^++k_2^+)}\\
S_{4,3} &= +\frac{2(k_2^++k_4^+)\Delta}{\sqrt{k_1^+k_2^+k_3^+k_4^+}}\frac{(\bar u_1 T^a\gamma^+ u_3)\ (\epsilon_2^\star iC^a\epsilon_4)}{(k_1^+-k_3^+)^2}\\
S_{6,1} &= +\frac{\Delta}{\sqrt{k_1^+k_2^+k_3^+k_4^+}}\frac{(\bar u_1 T^{a_3}\not\epsilon_3\gamma^+\not\epsilon_4 T^{a_4} v_2)}{(k_1^+-k_3^+)}\\
S_{6,2} &= -\frac{(k_3^+-k_4^+)\Delta}{\sqrt{k_1^+k_2^+k_3^+k_4^+}}\frac{(\bar u_1 T^a\,\gamma^+ v_2)\ (\epsilon_3 iC^a\epsilon_4)}{(k_1^++k_2^+)^2}\\
S_{7,1} &= -\frac{(k_1^++k_3^+)(k_2^++k_4^+)\Delta}{\sqrt{k_1^+k_2^+k_3^+k_4^+}}\ \frac{(\epsilon_1^\star C^a\epsilon_3)\ (\epsilon_2^\star C^a\epsilon_4)}{(k_1^+-k_3^+)^2}\\
S_{7,2} &= +\frac{2k_3^+k_4^+\Delta}{\sqrt{k_1^+k_2^+k_3^+k_4^+}}\ \frac{(\epsilon_1^\star C^a\epsilon_2^\star)\ (\epsilon_3 C^a\epsilon_4)}{(k_1^++k_2^+)^2}\\
S_{7,3} &= +\frac{\Delta}{\sqrt{k_1^+k_2^+k_3^+k_4^+}}\ (\epsilon_1^\star\epsilon_3)\ (\epsilon_2^\star\epsilon_4)\ C^a_{a_1a_2}C^a_{a_3a_4}\\
S_{7,4} &= +\frac{\Delta}{\sqrt{k_1^+k_2^+k_3^+k_4^+}}\ (\epsilon_1^\star\epsilon_3)\ (\epsilon_2^\star\epsilon_4)\ C^a_{a_1a_4}C^a_{a_3a_2}\\
S_{7,5} &= +\frac{\Delta}{\sqrt{k_1^+k_2^+k_3^+k_4^+}}\ (\epsilon_1^\star\epsilon_2^\star)\ (\epsilon_3\epsilon_4)\ C^a_{a_1a_3}C^a_{a_2a_4}
\end{aligned}
$$

Table 3: *The seagull interaction in terms of Dirac spinors. The matrix elements $S_{n,j}$ are displayed on the right, the corresponding (energy) graphs on the left. All matrix elements are proportional to $\Delta = \widetilde{g}^2\delta(k_1^+ + k_2^+|k_3^+ + k_4^+)\delta^{(2)}(\vec{k}_{\perp,1} + \vec{k}_{\perp,2}|\vec{k}_{\perp,3} + \vec{k}_{\perp,4})$, with $\widehat{g} = g/\sqrt{2(2\pi)^3}$. For periodic boundary conditions one uses $\widehat{g} = g/\sqrt{\Omega}$.*

and $\vec{P}$ are second-quantized Heisenberg operators. Unfortunately, this method is complicated by its non-covariant structure and the necessity to first understand its complicated vacuum eigenstate over all space and time. The presence of the square root operator presents severe mathematical difficulties. Even if these problems could be solved, the eigensolution is only determined in its rest system ($\vec{P} = 0$); determining the boosted wave function is as complicated as diagonalizing H itself. This is why instant form wave function cannot be applied in practice to scattering problems. Structure functions for example cannot be calculated.

In principle, the front form approach works in the same way. One aims at solving the Hamiltonian eigenvalue problem

$$H\,|\Psi\rangle = \frac{M^2 + \vec{P}_\perp^{\,2}}{P^+}\,|\Psi\rangle\,, \tag{14}$$

which for several reasons is easier: Contrary to P_z the operator P^+ is positive, having only positive eigenvalues. The square-root operator is absent. The boost operators are kinematic. Having determined the wave function in a particular frame with fixed total momenta P^+ and $\vec{P}_\perp$ the kinematic boost operators allow to covariantly transcribe to any other frame. In fact, as discussed below, one can formulate the theory frame-independently.

The ket $|\Psi\rangle$ can be calculated in terms of a complete set of functions $|\mu\rangle$ or $|\mu_n\rangle$,

$$\int d[\mu]\;\; |\mu\rangle\,\langle\mu| = \sum_n \int d[\mu_n]\;\; |\mu_n\rangle\,\langle\mu_n| = \mathbf{1}.$$

The transformation between the complete set of eigenstates $|\Psi\rangle$ and the complete set of basis states $|\mu_n\rangle$ are then $\langle\mu_n|\Psi\rangle$ and usually called the *wavefunctions* $\Psi_{n/h)}(\mu) \equiv \langle\mu_n|\Psi\rangle$. In addition to the quantum numbers of the Lorentz group, the eigenfunction is labeled by quantum numbers like charge, parity, or baryon number which specify a particular hadron h, thus

$$|\Psi\rangle = \sum_n \int d[\mu_n]\;\; |\mu_n\rangle\,\Psi_{n/h}(\mu).$$

One constructs the complete basis of Fock states $|\mu_n\rangle$ in the usual way by applying products of free field creation operators to the vacuum state $|0\rangle$:

$$\begin{array}{lll}
n=0: & |0\rangle\;, & \\
n=1: & \left|q\bar{q} : k_i^+, \vec{k}_{\perp i}, \lambda_i\right\rangle &= b^\dagger(q_1)\,d^\dagger(q_2)\;\;|0\rangle\;, \\
n=2: & \left|q\bar{q}g : k_i^+, \vec{k}_{\perp i}, \lambda_i\right\rangle &= b^\dagger(q_1)\,d^\dagger(q_2)\,a^\dagger(q_3)\;\;|0\rangle\;, \\
n=3: & \left|gg : k_i^+, \vec{k}_{\perp i}, \lambda_i\right\rangle &= a^\dagger(q_1)\,a^\dagger(q_2)\;\;|0\rangle\;, \\
\vdots & \vdots & \vdots \qquad\qquad \vdots\;\;|0\rangle\;.
\end{array}$$

The operators $b^\dagger(q)$, $d^\dagger(q)$ and $a^\dagger(q)$ create bare leptons (electrons or quarks), bare anti-leptons (positrons or antiquarks) and bare vector bosons (photons or

gluons). All of these particles are 'on-shell', $(k^\mu k_\mu)_i = m_i^2$. The various Fock-space classes are conveniently labeled with a running index n. Each Fock state $|\mu_n\rangle = |n : k_i^+, \vec{k}_{\perp i}, \lambda_i\rangle$ is an eigenstate of P^+ and $\vec{P}_\perp$ and the free part of the energy P_0^-, with eigenvalues

$$P^+ = \sum_{i\in n} k_i^+, \quad \vec{P}_\perp = \sum_{i\in n} \vec{k}_{\perp i}, \quad P_0^- = \sum_{i\in n} \frac{m_i^2 + k_{\perp i}^2}{k_i^+}.$$

The free invariant mass square of a Fock-state is $M_0^2 = (p_1 + p_2 + \ldots + p_{n_i})^2$, thus

$$M_0^2 = P_0^\mu P_{0,\mu} = P^+ P_0^- - \vec{P}_\perp^2 = P^+ \left(\sum_{i\in n} \frac{m_i^2 + k_{\perp i}^2}{k_i^+} \right) - \vec{P}_\perp^2. \tag{15}$$

The Fock and the physical vacuum have eigenvalues 0.

The restriction to $k^+ > 0$ is a key difference between light-cone quantization and ordinary equal-time quantization. In equal-time quantization, the state of a parton is specified by its ordinary three-momentum $\vec{k} = (k_x, k_y, k_z)$. Since each component of $\vec{k}$ can be either positive or negative, there exist zero total momentum Fock states of arbitrary particle number, and these will mix with the zero-particle state to build up the ground state, the physical vacuum. However, in light-cone quantization each of the particles forming a zero-momentum state must have vanishingly small k^+. The free or Fock space vacuum $|0\rangle$ is then an exact eigenstate of the full front form Hamiltonian H, in stark contrast to the quantization at equal usual-time. However, the vacuum in QCD is undoubtedly more complicated due to the possibility of color-singlet states with $P^+ = 0$ built on zero-mode massless gluon quanta, but the physical vacuum in the front form is *still far simpler* than in the usual instant form.

Since $k_i^+ > 0$ and $P^+ > 0$, one can define boost-invariant longitudinal momentum fractions

$$x_i = \frac{k_i^+}{P^+}\ , \qquad \text{with} \quad 0 < x_i < 1,$$

and boost-invariant intrinsic transverse momenta $\vec{k}_{\perp i}$ Their values are constrained,

$$\sum_{i\in n} x_i = 1 \quad \text{and} \quad \sum_{i\in n} \vec{k}_{\perp i} = \vec{0}, \tag{16}$$

corresponding to the intrinsic frame $\vec{P}_\perp = \vec{0}$. All particles in a Fock state $|\mu_n\rangle = |n : x_i, \vec{k}_{\perp i}, \lambda_i\rangle$ have a boosted four-momentum

$$p_i^\mu \equiv (p^+, \vec{p}_\perp, p^-)_i = \left(x_i P^+, \vec{k}_{\perp i} + x_i \vec{P}_\perp, \frac{m_i^2 + (\vec{k}_{\perp i} + x_i \vec{P}_\perp)^2}{x_i P^+} \right).$$

The free invariant mass square of the Fock state, Eq.(15), is therefore

$$M_0^2 = \sum_{i\in n} \left(\frac{m_i^2 + (\vec{k}_{\perp i} + x_i \vec{P}_\perp)^2}{x_i} \right) - \vec{P}_\perp^2 = \sum_{i\in n} \left(\frac{m^2 + \vec{k}_\perp^2}{x} \right)_i,$$

as a direct consequence of the transverse boost properties.

The phase-space differential $d[\mu_n]$ depends on how one normalizes the single particle states. In the convention where commutators are normalized to a Dirac-delta function, the phase space integration is

$$\begin{aligned}\int d[\mu_n]\ldots &= \sum_{\lambda_i\in n}\int\Big[dx_i d^2k_{\perp i}\Big]\ldots\ , \qquad \text{with}\\ \Big[dx_i d^2k_{\perp i}\Big] &= \delta\Big(1-\sum_{j\in n}x_j\Big)\delta^{(2)}\Big(\sum_{j\in n}\vec{k}_{\perp j}\Big)\ dx_1\ldots dx_{N_n}\ d^2k_{\perp 1}\ldots d^2k_{\perp N_n},\end{aligned}$$

where N_n is the number of particles in Fock state μ_n. The additional Dirac δ-functions account for the constraints (16). The eigenvalue equation (14) stands then for an infinite set of coupled integral equations

$$\begin{aligned}&\sum_{n'}\int[d\mu'_{n'}]\ \langle n: x_i,\vec{k}_{\perp i},\lambda_i|H|n': x'_i,\vec{k}'_{\perp i},\lambda'_i\rangle\ \Psi_{n'/h}(x'_i,\vec{k}'_{\perp i},\lambda'_i)\\ =\ &\frac{M^2+\vec{P}_\perp^{\,2}}{P^+}\Psi_{n/h}(x_i,\vec{k}_\perp,\lambda_i), \qquad \text{for}\quad n=1,\ldots,\infty.\end{aligned}\tag{17}$$

Since P^+ and $\vec{P}_\perp$ are diagonal operators one can rewrite this equation as

$$\begin{aligned}&\sum_{n'}\int[d\mu'_{n'}]\ \langle n: x_i,\vec{k}_{\perp i},\lambda_i|HP^+-\vec{P}_\perp^{\,2}|n': x'_i,\vec{k}'_{\perp i},\lambda'_i\rangle\ \Psi_{n'/h}(x'_i,\vec{k}'_{\perp i},\lambda'_i)\\ =\ &M^2\Psi_{n/h}(x_i,\vec{k}_\perp,\lambda_i).\end{aligned}\tag{18}$$

It is therefore possible to define a 'light-cone Hamiltonian' as the operator

$$H_{LC}=HP^+-\vec{P}_\perp^{\,2}=P^\mu P_\mu,\tag{19}$$

so that its eigenvalues correspond to the invariant mass spectrum M_i of the theory. Eq.(18) thus stands for

$$H_{LC}\,|\Psi\rangle=M^2\,|\Psi\rangle\,,\tag{20}$$

in analogy to Eq.(14).

The Lorentz invariance of H_{LC} and the boost invariance of the wave functions reflects the fact that the boost operators are kinematical. In fact one can boost the system to an 'intrinsic frame' in which the transversal momentum vanishes $\vec{P}_\perp=\vec{0}$, thus $H_{LC}=P^-P^+$. The transformation to an arbitrary frame with finite values of $\vec{P}_\perp$ is then trivially performed. Consider a pion in QCD with momentum $P=(P^+,\vec{P}_\perp)$ as an example. It is described by

$$|\pi:P\rangle=\sum_{n=1}^{\infty}\int d[\mu_n]\,\Big|n: x_iP^+,\vec{k}_{\perp i}+x_i\vec{P}_\perp,\lambda_i\Big\rangle\ \Psi_{n/\pi}(x_i,\vec{k}_{\perp i},\lambda_i),$$

where the sum is over all Fock space sectors of Eq.(15). The ability to specify wavefunctions simultaneously in any frame is a special feature of light-cone quantization. The light-cone wavefunctions $\Psi_{n/\pi}$ do not depend on the total momentum,

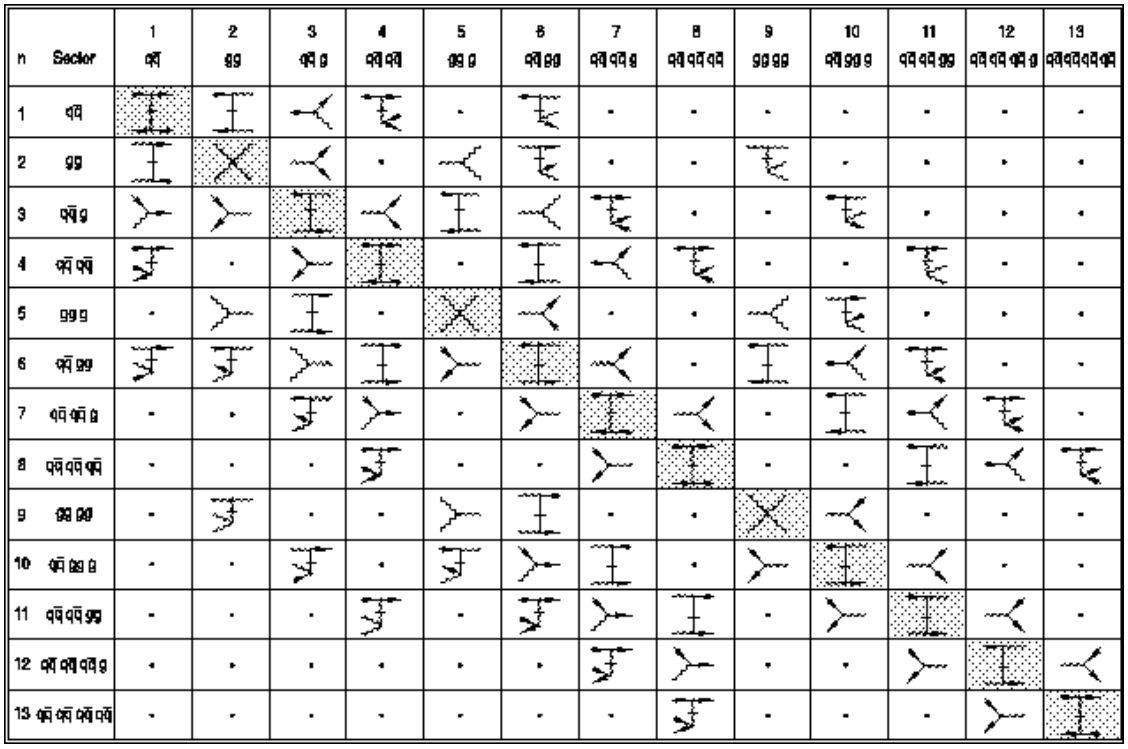

Figure 2: *The Hamiltonian matrix for a meson. The matrix elements are represented by energy diagrams. Within each block they are all of the same type: either vertex, fork or seagull diagrams. Zero matrices are denoted by a dot (·). The single gluon is absent since it cannot be color neutral.*

since x_i is the longitudinal momentum fraction carried by the i^{th} parton and $\vec{k}_{\perp i}$ is its momentum "transverse" to the direction of the meson; both of these are frame-independent quantities. They are the probability amplitudes to find a Fock state of bare particles in the physical pion. But given these light-cone wavefunctions $\Psi_{n/h}(x_i, \vec{k}_{\perp i}, \lambda_i)$, one can compute any hadronic quantity by convolution with the appropriate quark and gluon matrix elements, see for example [2].

In addressing to solve Eq.(20) one faces several major difficulties, among them that the above equations are ill-defined for very large values of the transversal momenta ('ultraviolet singularities') and for values of the longitudinal momenta close to the endpoints $x \sim 0$ or $x \sim 1$ ('endpoint singularities'). One has to introduce cut-offs Λ to regulate the theory in some convenient way. Subsequently one has to remove the cut-off dependence by renormalization group analysis. Renormalization theory is known however only for perturbation theory, for example when calculating Feynman scattering amplitudes in a certain order. Renormalization theory is not available for the bound-state problem. – But even if one has found a convenient regularization scheme, one faces the large (infinite) number of coupled

integral equations. Their nature resides in the complicated structure of the kernel

$$\langle n|H|n'\rangle \equiv \langle n : x_i, \vec{k}_{\perp i}, \lambda_i|H|n' : x_i', \vec{k}_{\perp i}', \lambda_i'\rangle.$$

In analyzing the structure of this very complicated many-body problem, as done in Figure 2, one realizes that most of its matrix elements are zero by nature of the operator structure of the Hamiltonian. The Hamiltonian is zero for all sectors whose particle number difference is larger than 2. As an example, consider the fork interaction given in Eq.(13) particularly its matrix element F_3. It scatters a quark into an other momentum state and distroys two gluons. In the block matrix element $\langle 1|H|6\rangle = \langle q\bar{q}|F_3|q\bar{q}\,gg\rangle$ one has many ways to realize that, without that the anti-quark $\bar{q}$ changes its momentum. In Fig. 2, all matrix elements in the block $\langle 1|H|6\rangle$ are therefore represented diagrammatically by the same energy diagram as in Table 2. Usually, the typical seagull matrix elements occur for the diagonal blocs of this matrix, with one exception: In the graph S_6 of Table 3 a $q\bar{q}$-pair is annihilated and scatteredg instantaneously into a gg-pair. Correspondingly, not all entries of the block matrix element $\langle 5|H|5\rangle = \langle q\bar{q}\,g|S_6|gg\,g\rangle$ can vanish. In order to cope with the formidable many-body problem imposed by Eq.(20), the method of discretized light-cone quantization is very useful.

3.1 Perturbation theory in the front form

Let us devote a section to the perturbative treatment of front-form gauge theory. Light-cone perturbation theory is really Hamiltonian perturbation theory, and we give the complete set of rules which are the analogues of the Feynman rules. We shall demonstrate in a selected example, that one gets the same covariant and gauge-invariant scattering amplitude as in Feynman theory, see also [2].

The Green's functions $\widehat{G}_{fi}(x^+)$ are the probability amplitudes that a state starting in Fock state $|i\rangle$ ends up in Fock state $|f\rangle$ at a later time x^+

$$\left\langle f \mid \widehat{G}(x^+) \mid i\right\rangle = \langle f|e^{-iP_+x^+}|i\rangle = i\int \frac{d\epsilon}{2\pi}\, e^{-i\epsilon x^+}\langle f|G(\epsilon)|i\rangle.$$

Its Fourier transform $\langle f \mid G(\epsilon) \mid i\rangle$ is called the resolvent of the Hamiltonian H, *i.e.*

$$\langle f \mid G(\epsilon) \mid i\rangle = \left\langle f\left|\frac{1}{\epsilon - H + i0_+}\right|i\right\rangle = \left\langle f\left|\frac{1}{\epsilon - H_0 - U + i0_+}\right|i\right\rangle.$$

Separating the Hamiltonian $H = H_0 + U$ into a free part H_0 and an interaction U, one can expand the resolvent into the series

$$\langle f|G(\epsilon)|i\rangle = \langle f|\widetilde{G}(\epsilon) + \widetilde{G}(\epsilon)U\widetilde{G}(\epsilon) + \widetilde{G}(\epsilon)U\widetilde{G}(\epsilon)U\widetilde{G}(\epsilon) + \ldots|i\rangle.$$

The rules for x^+-ordered perturbation theory follow when the resolvent of the free Hamiltonian $\widetilde{G}(\epsilon) = 1/(\epsilon - H_0 + i0_+)$ is replaced by its spectral decomposition

$$\widetilde{G}(\epsilon) = \sum_{n=1}^{\infty} \widetilde{G}_n(\epsilon), \quad \widetilde{G}_n(\epsilon) = \int d[\mu_n]\left|n : k_i^+, \vec{k}_{\perp i}, \lambda_i\right\rangle \frac{1}{\Delta_n}\left\langle n : k_i^+, \vec{k}_{\perp i}, \lambda_i\right|, \qquad (21)$$

with the energy denominator $\Delta_n = \epsilon - \sum_{i\in n}\left((k_\perp^2+m^2)/k^+\right)_i + i0_+$. The sum runs over all Fock states n intermediate between two interactions U.

To calculate then $\langle f|(\epsilon)|i\rangle$ perturbatively, all x^+-ordered diagrams must be considered, the contribution from each graph computed according to the rules of old-fashioned Hamiltonian perturbation theory [13, 14]:

1. Draw all topologically distinct x^+-ordered diagrams.

2. Assign to each line a single particle momentum k^μ, a helicity λ, as well as color and flavor. With fermions (electrons or quark) associate a spinor $u_\alpha(k,\lambda)$, with antifermions $v_\alpha(k,\lambda)$, and with vector bosons (photons or gluons) a polarization vector $\epsilon_\mu(k,\lambda)$.

3. For each vertex include the matrix element $\langle n|V|n'\rangle$ between Fock state n and n' as given in Table 1.

4. For each intermediate state there is an energy denominator $1/\Delta_n$ in which $\epsilon = P^-_{0,\rm in}$ is the incident free light-cone energy.

5. To account for three-momentum conservation include for each intermediate state the delta-functions $\delta\Big(P^+ - \sum_i k_i^+\Big)$ and $\delta^{(2)}\Big(\vec{P}_\perp - \sum_i \vec{k}_{\perp i}\Big)$.

6. Sum over all internal helicities (and colors for gauge theories) and integrate over each internal k with the weight $\int d^2k_\perp dk^+\theta(k^+)(2\pi)^{-3/2}$.

7. Include a factor -1 for each closed fermion loop, for each fermion line that both begins and ends in the initial state, and for each diagram in which fermion lines are interchanged in either of the initial or final states.

8. Imagine that every internal line is a sum of a 'dynamic' and an 'instantaneous' line, and draw all diagrams with $1, 2, 3, \ldots$ instantaneous lines.

9. Two consecutive instantaneous interactions give a vanishing contribution.

10. For each instantaneous line insert a factor $\langle n|W|n'\rangle$, with the matrix element given in Table 2 and 3.

The light-cone Fock state representation can thus be used advantageously in perturbation theory. The sum over intermediate Fock states is equivalent to summing all x^+-ordered diagrams and integrating over the transverse momentum and light-cone fractions x. Because of the restriction to positive x, diagrams corresponding to vacuum fluctuations or those containing backward-moving lines are eliminated.

3.2 The $q\bar{q}$-scattering amplitude

The simplest application of the above rules is the calculation of the electron-muon scattering amplitude to lowest non-trivial order. But the quark-antiquark scattering is only marginally more difficult. We thus imagine an initial $(q,\bar{q})$-pair with different flavors $f \neq \bar{f}$ to be scattered off each other by exchanging a gluon.

Let us treat this problem as a pedagogical example to demonstrate the rules. Rule 1: There are two time-ordered diagrams associated with this process. In the first one the gluon is emitted by the quark and absorbed by the antiquark, and in the second it is emitted by the antiquark and absorbed by the quark. For the first diagram, we assign the momenta required in rule 2 by giving explicitly the initial Fock state $|q,\bar{q}\rangle = \frac{1}{\sqrt{n_c}} \sum_{c=1}^{n_c} b^\dagger_{cf}(k_q,\lambda_q) d^\dagger_{c\bar{f}}(k_{\bar{q}},\lambda_{\bar{q}})|0\rangle$. Note that it is invariant under $SU(n_c)$. The final Fock state is $|q',\bar{q}'\rangle = \frac{1}{\sqrt{n_c}} \sum_{c=1}^{n_c} b^\dagger_{cf}(k'_q,\lambda'_q) d^\dagger_{c\bar{f}}(k'_{\bar{q}},\lambda'_{\bar{q}})|0\rangle$. The intermediate state

$$|q',\bar{q},g\rangle \;=\; \sqrt{\frac{2}{n_c^2-1}} \sum_{c=1}^{n_c} \sum_{c'=1}^{n_c} \sum_{a=1}^{n_c^2-1} T^a_{c,c'} b^\dagger_{c\bar{f}}(k'_q,\lambda'_q) d^\dagger_{c'\bar{f}}(k_{\bar{q}},\lambda_{\bar{q}}) a^\dagger_a(k_g,\lambda_g)|0\rangle \;, \quad (22)$$

has 'a gluon in flight'. Since the gluons longitudinal momentum is positive, the diagram allows only for $k'^+_q < k^+_q$. Rule 3 requires at each vertex the factors

$$\langle q,\bar{q}|\, V \,|q',\bar{q},g\rangle \;=\; \frac{g}{(2\pi)^{\frac{3}{2}}} \sqrt{\frac{n_c^2-1}{2n_c}} \; \frac{\left[\overline{u}(k_q,\lambda_q)\,\gamma^\mu \epsilon_\mu(k_g,\lambda_g)\,u(k'_q,\lambda'_q)\right]}{\sqrt{2k^+_q}\sqrt{2k^+_g}\sqrt{2k'^+_q}} \;, \quad (23)$$

$$\langle q',\bar{q},g|\, V \,|q',\bar{q}'\rangle \;=\; \frac{g}{(2\pi)^{\frac{3}{2}}} \sqrt{\frac{n_c^2-1}{2n_c}} \; \frac{\left[\overline{v}(k'_{\bar{q}},\lambda'_{\bar{q}})\,\gamma^\nu \epsilon^\star_\nu(k_g,\lambda_g)\,v(k_{\bar{q}},\lambda_{\bar{q}})\right]}{\sqrt{2k^+_{\bar{q}}}\sqrt{2k^+_g}\sqrt{2k'^+_{\bar{q}}}}, \quad (24)$$

respectively, wich are found by means of Table 1. Working with color neutral Fock states, all color structure reduces to an overall factor C, with $C^2 = (n_c^2 - 1)/2n_c$. Rule 4 requires the energy denominator $1/\Delta_3$. It is useful to work the four-momentum transfers of the quark $Q^2 = -(k_q - k'_q)^2 = k^+_g(k_g + k'_q - k_q)^-$. The anti-quark has $\overline{Q}^2 = (k_{\bar{q}} - k'_{\bar{q}})^2 = k^+_g(k_g + k_{\bar{q}} - k'_{\bar{q}})^-$. With the initial energy $\epsilon = \widetilde{P}_+ = (k_q + k_{\bar{q}})_+ = \frac{1}{2}(k_q + k_{\bar{q}})^-$, the energy denominator becomes then

$$\Delta_3 = (k_q + k_{\bar{q}})^- - (k_g + k'_q + k_{\bar{q}})^- = -\frac{Q^2}{k^+_g}$$

Rule 5 requires two Dirac-delta functions, one at each vertex, to account for conservation of three-momentum. One of them is removed by the requirement of rule 6, namely to integrate over all intermediate internal momenta and the other remains in the final equation (26). The gluon momentum is thus fixed by the external legs of the graph. The polarization sum over the gluon helicity gives

$$d_{\mu\nu}(k_g) \equiv \sum_{\lambda_g} \epsilon_\mu(k_g,\lambda_g)\,\epsilon^\star_\nu(k_g,\lambda_g) = -g_{\mu\nu} + \frac{k_{g,\mu}\eta_\nu + k_{g,\nu}\eta_\mu}{k^\kappa_g \eta_\kappa}.$$

The null vector has the components $\eta^\mu = (\eta^+, \vec{\eta}_\perp, \eta^-) = (0, \vec{0}_\perp, 2)$ and thus the properties $\eta^2 \equiv \eta^\mu \eta_\mu = 0$ and $k\eta = k^+$. As shown explicitly in [2] one gets for the second order diagram $\langle q, \bar{q}|V\widetilde{G}_3 V|q', \bar{q}'\rangle$ after some non-trivial steps

$$\langle q, \bar{q}|V\widetilde{G}_3 V|q', \bar{q}'\rangle = \frac{g^2C^2}{(2\pi)^3} \frac{\left[\overline{u}(k_q, \lambda_q)\gamma^\mu u(k'_q, \lambda'_q)\right]}{\sqrt{4k_q^+ k_q'^+}} \frac{1}{Q^2} \frac{\left[\overline{u}(k_{\bar{q}}, \lambda_{\bar{q}})\gamma_\mu u(k'_{\bar{q}}, \lambda'_{\bar{q}})\right]}{\sqrt{4k_{\bar{q}}^+ k_{\bar{q}}'^+}}$$
$$-\frac{g^2C^2}{(2\pi)^3} \frac{\left[\overline{u}(k_q, \lambda_q)\gamma^+ u(k'_q, \lambda'_q)\right]}{\sqrt{4k_q^+ k_q'^+}} \frac{1}{(k_g^+)^2} \frac{\left[\overline{u}(k_{\bar{q}}, \lambda_{\bar{q}})\gamma^+ u(k'_{\bar{q}}, \lambda'_{\bar{q}})\right]}{\sqrt{4k_{\bar{q}}^+ k_{\bar{q}}'^+}}. \quad (25)$$

The delta-functions and a step function $\Theta(k_q'^+ \leq k_q^+)$ are omitted for simplicity. One proceeds with rule 8, by including the instantaneous lines. Table 3 gives

$$\langle q, \bar{q}|\, S\, |q', \bar{q}'\rangle = \frac{g^2C^2}{(2\pi)^3} \frac{\left[\overline{u}(k, \lambda)\gamma^+ u(k', \lambda')\right]_q}{\sqrt{4k_q^+ k_q'^+}} \frac{1}{(k_q^+ - k_q'^+)^2} \frac{\left[\overline{u}(k, \lambda)\gamma^+ u(k', \lambda')\right]_{\bar{q}}}{\sqrt{4k_{\bar{q}}^+ k_{\bar{q}}'^+}}.$$

The $q\bar{q}$-scattering amplitude, the sum $\langle q, \bar{q}|\, S + V\widetilde{G}_3 V\, |q', \bar{q}'\rangle$ has then the correct gauge-invariant result known from Feynman theory up to second order

$$\begin{aligned}\langle q, \bar{q}|S + V\widetilde{G}_3 V|q', \bar{q}'\rangle &= \frac{(-1)}{(k_q - k'_{\bar{q}})^2} \frac{1}{\sqrt{k_q^+ k_{\bar{q}}^+ k_q'^+ k_{\bar{q}}'^+}} \delta(P^+ - P'^+)\delta^{(2)}(\vec{P}_\perp - \vec{P}'_\perp) \\ &\times \frac{(gC)^2}{(2\pi)^3} \left[\overline{u}(k, \lambda)\gamma^\mu u(k', \lambda')\right]_q \left[\overline{u}(k, \lambda)\gamma_\mu u(k', \lambda')\right]_{\bar{q}}. \quad (26)\end{aligned}$$

The instantaneous diagram is cancelled exactly.

4 Discretized Light-Cone Quantization

The infinitely many coupled integral equations in the preceeding section a very difficult to cope with in practice. Because of the many integrations and summations it is very difficult to even write them down. But field theory becomes much more transparent when one works with periodic boundary conditions. The coupled integral equations become then coupled matrix equations. Since rows and colums of a matrix can be denumerated, one can keep track of the necessary manipulations much easier. In fact, working with periodic boundary conditions, or with 'Discretized Light-Cone Quantization' (DLCQ), one has obtained the first total solutions to non-trivial quantum field theories in 1+1 dimensions. In 3+1 dimensions the method has the ambitious goal to calculate the spectra and wavefunctions of physical hadrons from a covariant gauge field theory. The ingredients of the method shall be reviewed in short in this section.

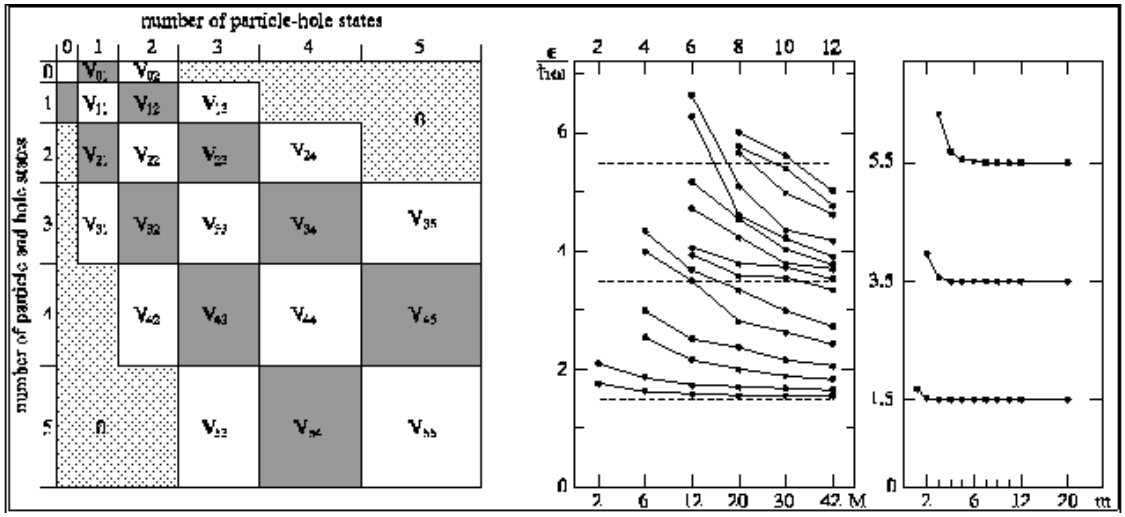

Figure 3: *Non-relativistic many-body theory.*

4.1 The non-relativistic A-body problem in one dimension

Let us first briefly review the difficulties for a conventional non-relativistic many-body theory. One starts with a many-body Hamiltonian $H = T + U$. The kinetic energy T is usually a one-body operator and thus simple. The potential energy U is at least a two-body operator and thus complicated. One has solved the problem if one has found the eigenvalues and eigenfunctions of the Hamiltonian equation, $H\Psi = E\Psi$. One always can expand the eigenstates in terms of products of single particle states $\langle \vec{x}|m\rangle$ belonging to a complete set of ortho-normal functions. When antisymmetrized, one refers to them as 'Slater-determinants'. All Slater-determinants with a fixed particle number form a complete set.

One can proceed as follows. In the first step one chooses a complete set of single particle wave functions. These single particle wave functions are solutions of an arbitrary single particle Hamiltonian. In a second step, one selects one Slater determinat as a reference state. All Slater determinants can be classified relative to this reference state as 1-particle-1-hole (1-ph) states, 2-particle-2-hole (2-ph) states, and so on. The Hilbert space is truncated at some level. In a third step, one calculates the Hamiltonian matrix within this Hilbert space.

In Figure 3, the Hamiltonian matrix for a two-body interaction is displayed schematically. Most of the matrix-elements vanish, since a 2-body Hamiltonian changes the state by up to 2 particles. Therefore the structure of the Hamiltonian is a finite penta-diagonal block matrix. The dimension within a block is made finite by an artificial cut-off on the kinetic energy, *i.e.* on the single particle quantum numbers m. A finite matrix can be diagonalized on a computer. At the end one must verify that the physical results are reasonably insensitive to the cut-off(s) and other formal parameters.

This procedure was actually carried out in one space dimension [15] with two

different sets of single-particle functions,

$$\langle x|m\rangle = N_m H_m\Big(\frac{x}{L}\Big)\exp\Big\{-\frac{1}{2}\Big(\frac{x}{L}\Big)^2\Big\} \qquad \text{and} \quad \langle x|m\rangle = N_m \exp\Big\{im\frac{x}{L}\pi\Big\}\ . \quad (27)$$

The two sets are the eigenfunctions of the harmonic oscillator ($L \equiv \hbar/m\omega$) with its Hermite polynomials H_m, and the eigenfunctions of the momentum of a free particle with periodic boundary conditions. Both are suitably normalized (N_m), and both depend parametrically on a characteristic length parameter L. The calculations are particularly easy for particle number 2, and for a harmonic two-body interaction. The results are displayed in Figure 3, and surprisingly different. For the plane waves, the results converge rapidly to the exact eigenvalues $E = \frac{3}{2}, \frac{7}{2}, \frac{11}{2}, \ldots$, as shown in the right part of the figure. Opposed to this, the results with the oscillator states converge extremely slowly. Obviously, the larger part of the Slater determinants is wasted on building up the plane wave states of center of mass motion from the Slater determinants of oscillator wave functions. It is obvious, that the plane waves are superior, since they account for the symmetry of the problem, namely Galilean covariance. The approach was successfully applied for getting the exact eigenvalues and eigenfunctions for up to 30 particles.

From these calculations, one should conclude that discretized plane waves are a useful tool for many-body problems, and that the generate good wavefunctions even for a 'confining' potential like the harmonic oscillator.

4.2 QED in 1+1 dimension

DLCQ had been applied first to Yukawa theory [16] in 1-space and 1-time dimensions followed by an application to QED [17] and to QCD [18], but the advantages of working with periodic boundary conditions in the front form, particularly when discussing the 'zero modes' in the ϕ^4-theory, had been noted also by Maskawa and Yamawaki [26] in 1976.

In one space dimension are no rotations — hence no spin. The Dirac spinor has two components and the Dirac matrices are 2 by 2 matrices. The gauge field A^μ field has two components. One of them is eliminated by fixing the gauge, and the other determined by Gauss' law. The gauge field carries no dynamical degree of freedom. The theory confines quarks (or electrons) because the Poisson equation in 1 space dimension gives rise to a linearly rising potential.

Quantum electrodynamics in 1+1 dimension has played an important role in field theory because its massless version, the Schwinger model, is analytically soluable. The fundamental solution corresponds to a composite $e\bar{e}$-state – the Schwinger-boson – with invariant mass $m_B \equiv g/\sqrt{\pi}$. Note that the coupling constant g in 1+1 dimension has the dimension of a mass.

Consider first the massive Schwinger model. The Lagrangian for the theory takes the same form as in Eq.(3). Again one works in the light-cone gauge $A^+ = 0$, and uses the same projection operators $\Lambda_\pm$. The Dirac equation decomposes again

Sector	n	1	2	3	4	5	6	7	8
$q\bar{q}$	1	D	F	·	·	·	·	·	·
$q\bar{q}\,q\bar{q}$	2	F	D	F	·	·	·	·	·
$q\bar{q}\,q\bar{q}\,q\bar{q}$	2	·	F	D	F	·	·	·	·
$q\bar{q}\,q\bar{q}\,q\bar{q}\,q\bar{q}$	4	·	·	F	D	F	·	·	·
5 $q\bar{q}$-pairs	5	·	·	·	F	D	F	·	·
6 $q\bar{q}$-pairs	6	·	·	·	·	F	D	F	·
7 $q\bar{q}$-pairs	7	·	·	·	·	·	F	D	F
8 $q\bar{q}$-pairs	8	·	·	·	·	·	·	F	D

Table 4: *Fock-space sectors and block matrix structure for QED in 1+1 dimension. Diagonal blocs (D=T+S) refer to seagull, off-diagonal (F) to fork matrix elements. A zero block matrix is marked by (·).*

into a time-derivative $2i\partial^+\Psi_+ = m\beta\Psi_- + gA^-\Psi_+$ and a constraint $2i\partial^-\Psi_- = m\beta\Psi_+$. One is left with only one independent field, Ψ_+, which is canonically quantized at $x^+ = 0$,

$$\{\Psi_+(x^-,x^+),\Psi_+^\dagger(y^-,y^+)\}_{x^+=y^+=0} = \Lambda_+\delta(x^- - y^-). \tag{28}$$

The formalism gets somewhat simplified if one uses the chiral representation [18]

$$\gamma^0 = \begin{pmatrix} 0 & 1 \\ 1 & 0 \end{pmatrix}, \quad \gamma^1 = \begin{pmatrix} 0 & 1 \\ -1 & 0 \end{pmatrix}, \quad \gamma^5 = \gamma^0\gamma^1 = \begin{pmatrix} -1 & 0 \\ 0 & 1 \end{pmatrix}.$$

The $\Lambda_\pm = (1 \pm \gamma^0\gamma^1)/2$ are then diagonal and project on the chiral components

$$\Psi = \begin{pmatrix} \Psi_L \\ \Psi_R \end{pmatrix}, \quad \Psi_+ = \begin{pmatrix} 0 \\ \Psi_R \end{pmatrix}, \quad \Psi_- = \begin{pmatrix} \Psi_L \\ 0 \end{pmatrix}.$$

The (light-cone) momentum and energy operators become

$$\begin{aligned} P^+ &= \int_{-L}^{+L} dx^- \Psi_R^\dagger \partial_- \Psi_R, \\ P^- &= m^2 \int_{-L}^{+L} dx^- \Psi_R^\dagger \frac{1}{i\partial_-}\Psi_R + \frac{g^2}{2}\int_{-L}^{+L} dx^- \Psi_R^\dagger\Psi_R \frac{1}{(i\partial_-)^2}\Psi_R^\dagger\Psi_R. \end{aligned}$$

One can expand Ψ_R (or Ψ_+) with periodic boundary conditions [17], but anti-periodic boundary conditions [18] avoid the zero mode:

$$\Psi_R(x^-) = \frac{1}{\sqrt{2L}} \sum_{n=\frac{1}{2},\frac{3}{2},\ldots}^{\infty} \left(b_n e^{-i\frac{n\pi}{L}x^-} + d_n^\dagger e^{i\frac{n\pi}{L}x^-} \right).$$

The creation and destruction operators obey $\left\{b_n^\dagger, b_m\right\} = \left\{d_n^\dagger, d_m\right\} = \delta_{n,m}$, consistent with Eq.(28). One redefines units by

$$P^+ = \frac{2\pi}{L}K, \quad P_0^- = \frac{L}{2\pi}\left(m^2\,H_0 + \frac{g^2}{\pi}\,U\right).$$

1	$\frac{1}{2};\frac{7}{2}$
2	$\frac{3}{2};\frac{5}{2}$
2	$\frac{5}{2};\frac{3}{2}$
4	$\frac{7}{2};\frac{1}{2}$
5	$\frac{1}{2},\frac{3}{2};\frac{1}{2},\frac{3}{2}$

Table 5: *The 5 Fock states for $K = 4$.*

K	1 $q\bar{q}$	2 $q\bar{q}$	3 $q\bar{q}$	4 $q\bar{q}$	Total
1	1	-	-	-	1
4	4	1	-	-	5
9	9	20	1	-	30
16	16	140	74	1	231

Table 6: *Number of Fock states versus harmonic resolution.*

The length L drops out in $H_{\rm LC} = P^+P^-$. Inserting the above fields gives

$$
\begin{aligned}
K &= \sum_{n=\frac{1}{2},\frac{3}{2},\ldots}^{\infty} n\left(b_n^\dagger b_n + d_n^\dagger d_n\right), \quad H_0 = \sum_{n=\frac{1}{2},\frac{3}{2},\ldots}^{\infty} \frac{1}{n}\left(b_n^\dagger b_n + d_n^\dagger d_n\right), \\
U &= :U: + \sum_{n=\frac{1}{2},\frac{3}{2},\ldots}^{\infty} \frac{I_n}{n}\left(b_n^\dagger b_n + d_n^\dagger d_n\right), \quad \text{with} \quad I_n = -\frac{1}{2n} + \sum_{m=1}^{n+\frac{1}{2}} \frac{1}{m^2}, \\
:U: &= \sum_{n_1,n_2,n_3,n_4} \frac{\delta(n_1+n_2|n_3+n_4)}{2(n_1-n_3)^2}\left(b_1^\dagger b_2^\dagger b_3 b_4 + d_1^\dagger d_2^\dagger d_3 d_4\right) \\
&+ \sum_{n_1,n_2,n_3,n_4} \delta(n_1+n_2|n_3+n_4)\left(\frac{1}{(n_1-n_3)^2} - \frac{1}{(n_1+n_2)^2}\right) b_1^\dagger d_2^\dagger b_3 d_4 \\
&+ \sum_{n_1,n_2,n_3,n_4} \frac{\delta(n_1|n_2+n_3+n_4)}{(n_1-n_3)^2}\left(b_1^\dagger b_2 b_3 d_4 + d_1^\dagger d_2 d_3 b_4 + h.c.\right).
\end{aligned}
$$

The symbols $\delta(n|m) = \delta_{n,m}$ are Kronecker delta's and $b_1 \equiv b_{n_1}$. In 1+1 dimensions it is very important to keep the 'self-induced inertias' I_n from the normal ordering. They are needed to cancel the infrared singularity in the interaction term in the continuum limit.

The next step is to actually solve the equations of motions in the discretized space. Typically one proceeds as follows: One constructs the Fock space

$$|\mu_n\rangle = |q_1,\ldots,q_n;\bar{q}_1,\ldots,\bar{q}_n\rangle = b_{q_1}^\dagger,\ldots,b_{q_n}^\dagger d_{\bar{q}_1}^\dagger,\ldots,d_{\bar{q}_n}^\dagger|0\rangle,$$

in the same way as above in Eq.(15), and arranges it in denumerated Fock space sectors, as illustrated in Table 4. Each Fock state must be an eigenstate to P^+ and thus of the *harmonic resolution* K [17], with eigenvalue $K = \sum_{i\in\mu_n} n_i$. One selects now one value for K and constructs all Fock states. Both the number of Fock space sectors and the number of Fock states within each sector are finite for every finite K, due to the positivity condition on the light-cone momenta. For $K = 1$ one has only one Fock-space class with one Fock state $|\frac{1}{2};\frac{\bar{1}}{2}\rangle = b_{\frac{1}{2}}^\dagger d_{\frac{1}{2}}^\dagger|0\rangle$, for $K = 4$ one has the 5 Fock states given in Table 5. The numbers of Fock states increase with given K, as shown in Table 6, but less than exponentially due to the exclusion

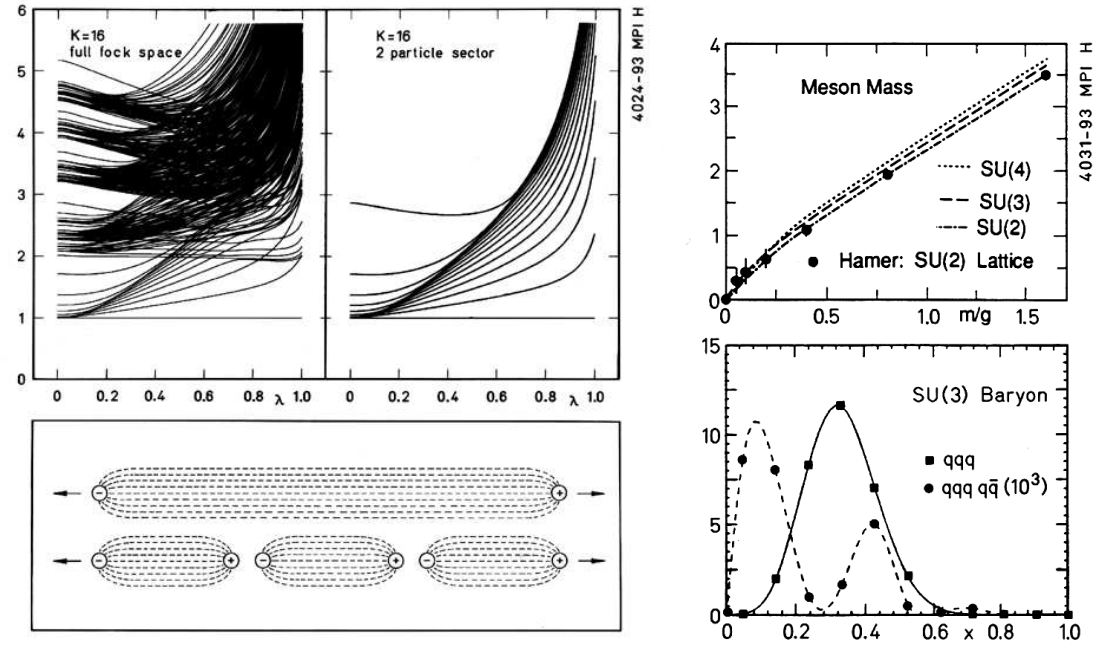

Figure 4: *Spectra and wavefunctions in 1+1 dimensions, taken from [17, 18].*

principle. Next, one calculates the matrix elements of $H = P^-$. In the last step one diagonalizes H. Any of its eigenvalues $E(K)$ depends on K and corresponds to an invariant mass $M^2(K) \equiv P^+P^- = KE(K)$. Notice that one gets a spectrum of invariant mass-squares for any value of K.

The eigenvalue spectrum of QED$1+1$ was given first by Eller [17], for periodic boundary conditions on the fermion fields. The plot likeon the left side in Figure 4 was calculated [22] with anti-periodic boundary conditions. It shows the full mass spectrum of QED in the charge zero sector for all values of the coupling constant and the fermion mass, parametrized by $\lambda = (1 + \pi(m/g)^2)^{-\frac{1}{2}}$. The eigenvalues M_i are plotted in units where the mass of the lowest 'positronium' state has the numerical value 1. All states with $M > 2$ are unbound. The plot includes the free case $\lambda = 0$ ($g = 0$) and the the Schwinger limit $M = 1$ for $\lambda = 1$ ($m = 0$), where DLCQ generates the exact eigenvalue. – The lower left part of the figure illustrates the following point. The rich complexity of the spectrum allows for multi-particle Fock states *at the same invariant mass* as the 'simple $q\bar{q}$-states' shown in the figure as the '2 particle sector'. The spectrum includes not only the simple bound state spectrum, but also the associated discretized continuum of the same particles in relative motion. One can identify the simple bound states as two quarks connected by a confining string as displayed in the figure. The smallest residual interaction mixes the simple configuration with the large number of 'continuum states' at the same mass. The few simple states have a much smaller statistical weight, and it

looks as if the long string 'breaks' into several pieces of smaller strings. Loosely speaking one can interpret such a process as the decay of an excited pion into multi-pion configurations $\pi^\star \to \pi\pi\pi$.

In 1+1 dimensions quantum electro dynamics [17] and quantum chromo dynamics [18] show many similarities, both from the technical and from the phenomenological point of view. In the right part of Figure 4 some of the results of Hornbostel [18] on the spectrum and the wavefunctions for QCD are displayed. Fock states in non-abelian gauge theory SU(N) can be made color singlets for any order of the gauge group and thus one can calculate mass spectra for mesons and baryons for almost arbitrary values of N. In the upper right part of the figure the lowest mass eigenvalue of a meson is given for $N = 2, 3, 4$. Lattice gauge calculations are available only for $N = 2$ and for the lowest two eigenstates [19]. In general the agreement is very good. In the left lower part of the figure the structure function of a baryon is plotted versus (Bjørken-)x for $m/g = 1.6$. With DLCQ it is possible to calculate also higher Fock space components. As an example, the figure includes the probability distribution to find a quark in a $qqq\,q\bar{q}$-state.

4.3 Fermion condensates and the small mass limit

Based on the low energy theorems from times prior to QCD, it is believed that the square of the pion mass is linear in the quark mass m for sufficiently small m. The proportionality constant has to have a dimension of mass, and since there is no other scale in the problem except the *quark condensates in the vacuum* $\langle 0|\overline{\Psi}\Psi|0\rangle$, one believes that the square of the pion mass is approximatively given by $m_\pi^2 \sim 2\langle 0|\overline{\Psi}\Psi|0\rangle m$, a theorem which was succesful in many phenomenological applications.

The Schwinger model has played an important role as a paradigm for our understanding of hadronic physics. Among other aspects it has the desired feature that the invariant mass square of the $e\bar{e}$-boson is linear in the electron mass m

$$M^2 = m_B^2 + 2m\,\langle 0|\overline{\Psi}\Psi|0\rangle, \quad \text{with} \quad \langle 0|\overline{\Psi}\Psi|0\rangle = e^\gamma\; m_B, \tag{29}$$

where $m_B \equiv g/\sqrt{\pi}$ is the invariant mass in the Schwinger limit. Euler's constant γ was understood as a signal for non-perturbative physics. In his analysis of the Schwinger model, Bergknoff [20] showed that the take-off from the Schwinger limit obeys

$$\langle 0|\overline{\Psi}\Psi|0\rangle = \frac{\pi}{\sqrt{3}}\; m_B. \tag{30}$$

The result of this 'chiral perturbation theory' to first order, $\frac{\pi}{\sqrt{3}} \sim 1.81$, is numerically very close to $e^\gamma \sim 1.78$.

Its is actually quite easy to derive the Bergknoff equation from DLCQ [21]. For a fixed resolution K, a $q\bar{q}$-state is fixed by the quantum number n of the electron.

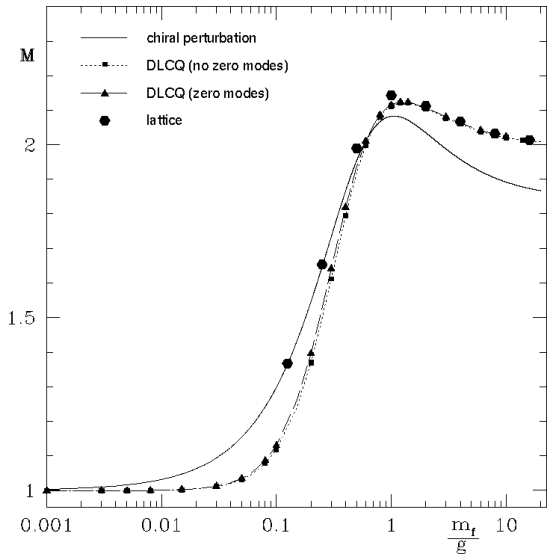

Figure 5: *The lowest mass eigenvalue of QED_{1+1} in units of m_B is plotted versus the fermion mass m_f in units of the coupling constant g, as calculated with 'conventional DLCQ' ($K = 16$). Taken from Ref. [23]. See also discussion in the text.*

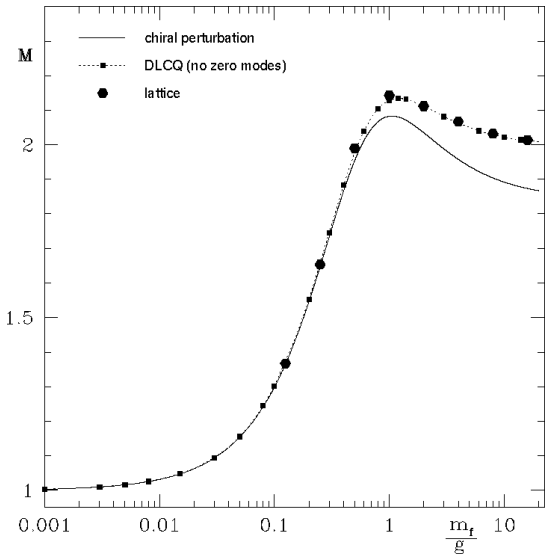

Figure 6: *The lowest mass eigenvalue of QED_{1+1} in units of m_B is plotted versus the fermion mass m_f in units of the coupling constant g, as calculated with 'improved DLCQ' ($K = 20$), as proposed in Ref. [25]. Taken from Ref. [23]. See also discussion in the text.*

The eigenvalue equation is then given by

$$M^2\langle n|\Psi\rangle = \sum_{n'=\frac{1}{2}}^{[K]} \langle n|H_{LC}|n'\rangle\,\langle n'|\Psi\rangle, \quad \text{for} \quad n = \frac{1}{2}, \frac{3}{2}, \ldots, \, [K],$$

with $[K] \equiv K - \frac{1}{2}$. Using the Hamiltonian matrix elements are given above, one introduces $x = p^+/P^+ = n/K$ and goes to the continuum limit. After a few steps [21] one gets the integral equation of Bergknoff [20],

$$M^2\langle x|\Psi\rangle = \frac{m^2}{x(1-x)}\langle x|\Psi\rangle + m_B^2 \int_0^1 dx'\langle x'|\Psi\rangle + m_B^2 \int\!\!\!\!\!\!- \, dx' \frac{\langle x|\Psi\rangle - \langle x'|\Psi\rangle}{(x-x')^2}.$$

For $m = 0$, the solution $\langle x|\Psi\rangle = 1$ has the eigenvalue $M^2 = m_B^2$, the Schwinger boson.

Eqs.(29) and (30) state that the mass-squared of the Schwinger boson is *linear in the fermion mass* m, in the limit when m goes to zero. For a long time, this result was in conflict with the explicit DLCQ-calulations [17, 22, 23]. The shortcoming was taken as a hint [24] that light-cone quantization was in failure because of the trivial vacuum structure which does not allow for condensates.

The most recent results by Völlinger [23] for DLCQ are displayed in Figure 5. They are compared with the lattice calculations of Crewther and Hamer [19] and with chiral perturbation theory up to second order [24]. The lattice results and DLCQ show some discrepancy for very small m which however fades away for larger m. On the other hand, the lattice results and chiral perturbation theory agree perfectly at small and deviate for large m, where chiral perturbation theory is not suposed to work. The figure show aslo that a correct inclusion of the (gauge field) zero modes has no significant impact. The re-solution of this puzzle came by van de Sande [25]. He realized that conventional DLCQ has difficulties to reproduce the wave function $\langle x|\Psi\rangle$ near the endpoints $x \to 0$ and $x \to 1$ very close to the Schwinger limit. His 'improved DLCQ' accounts for that, and indeed when properly included as shown in Figure 6 all discrepancies fade away.

What should be learned from this exercise is that not everything what is called a 'vacuum condensate' in the literature deserves this name in a physical sense: In naive light-cone quantization particularly DLCQ the vacuum is trivial and can not have condensates.

4.4 Φ^4 in 1+1 dim's: Zero modes and phase transitions

The naive front-form vacuum is simple. However, one commonly associates important long range properties of a field theory with the vacuum like spontaneous symmetry breaking, the Goldstone pion, or color confinement. If one cannot associate long range phenomena with the vacuum state itself, then the only alternative is the zero momentum components of the field, the 'zero modes'. In some cases, the zero mode operator is not an independent degree of freedom but obeys a constraint equation. Consequently, it is a complicated operator-valued function of all the other modes of the field. Zero modes of this type have been investigated first by Maskawa and Yamawaki as early as in 1976 [26]. An analysis of the zero mode constraint equation for (1+1)–dimensional ϕ^4 field theory, by van de Sande and Pinsky [27], shows how spontaneous symmetry breaking occurs within the context of this model.

The model represents a new paradigm for spontaneous symmetry breaking and shall be reviewed shortly. The Lagrangian in one space and one time dimension is $\mathcal{L} = \partial_+\phi\partial_-\phi - \frac{\mu^2}{2}\phi^2 - \frac{\lambda}{4!}\phi^4$. Imposing periodic boundary conditions with a length parameter $d = 2L$ gives $\phi(x) = \frac{1}{\sqrt{d}}\sum_{n=-\infty}^{\infty} q_n(x^+)e^{i\frac{\pi}{L}nx^-}$. The field integral $\Sigma_n = \int dx^-\,\phi(x)^n - (zero\ modes)$ is convenient to discuss the problem and becomes

$$\Sigma_n = \frac{1}{n!}\sum_{i_1,i_2,\ldots,i_n\neq 0} q_{i_1}q_{i_2}\ldots q_{i_n}\,\delta_{i_1+i_2+\ldots+i_n,0}.$$

Also the canonical Hamiltonian can be disentangled into Σ_n and the zero mode q_0

$$P^- = \frac{\mu^2}{2}q_0^2 + \mu^2\Sigma_2 + \frac{\lambda}{4!d}q_0^4 + \frac{\lambda}{2!d}q_0^2\Sigma_2 + \frac{\lambda}{d}q_0\Sigma_3 + \frac{\lambda}{d}\Sigma_4.$$

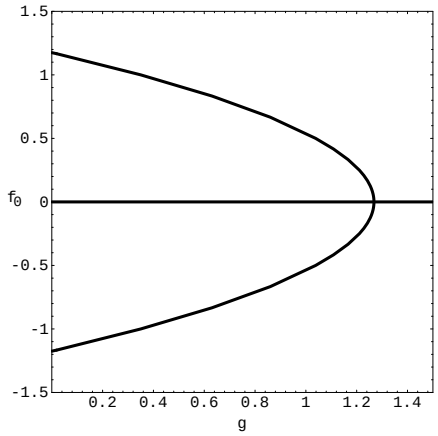

Figure 7: *The vacuum expectation value of ϕ, $f_0 = \sqrt{4\pi}\langle 0|\phi|0\rangle$ is plotted versus $g = 24\pi\mu^2/\lambda$, which is the inverse of the coupling constant λ. Taken from [27]. — In the front form, the vacuum state $|0\rangle$ is simple, but the operator ϕ, or a_0, is complicated. In the conventional instant form, the vacuum $|0\rangle$ is complicated but the operator ϕ is simple.*

One can apply canonical quantization. Following the Dirac-Bergman prescription, described in [2], one identifies first-class constraints which define the conjugate momenta $0 = p_n - ik_n^+ q_{-n}$,, where $[q_m, p_n] = \delta_{n,m}/2$ and $m, n \neq 0$. The secondary constraint

$$0 = \mu^2 q_0 + \frac{\lambda}{3!d} q_0^3 + \frac{\lambda}{d} q_0 \Sigma_2 + \frac{\lambda}{d} \Sigma_3 \tag{31}$$

determines the zero mode q_0. This result can also be obtained by integrating the equations of motion, $\partial_+\partial_-\phi + \mu^2\phi = \frac{\lambda}{3!}\phi^3$. To quantize the system one replaces the Dirac bracket by a commutator. One must choose a regularization and an operator-ordering prescription in order to make the system well-defined. One begins by defining creation and annihilation operators $a_k^\dagger$ and a_k,

$$q_k = \sqrt{\frac{d}{4\pi\,|k|}}\, a_k \ , \quad a_k = a_{-k}^\dagger \ , \quad k \neq 0 \ ,$$

which satisfy the usual commutation relations $\left[a_k, a_l^\dagger\right] = \delta_{k,l}$. Likewise, one defines the zero mode operator $q_0 = a_0\sqrt{d/4\pi}$. In the quantum case, one normal orders the operator Σ_n. One redefines this the fields in terms of operators

$$\phi(x) = \frac{1}{\sqrt{d}} \left(a_0 + \sum_{n=1}^{\infty} \frac{1}{n} \left(a_n e^{-i\frac{\pi}{L}nx^-} + a_n^\dagger e^{i\frac{\pi}{L}nx^-} \right) \right), \tag{32}$$

and notes that they obey the canonical commutation relations

$$\left[\phi(x^+, x^-), \partial_-\phi(y^+, y^-)\right]_{x^+=y^+=0} = \delta(x^- - y^-), \tag{33}$$

for a boson field in the front form, see also Eq.(28).

The solution of the constraint Eq.(31) is very difficult. Van de Sande and Pinsky [27] have shown that the zero mode a_0 could acquire finite values,

$$\langle 0|\phi|0\rangle = a_0 \neq 0,$$

depending on the coupling constant.

One finds the following general behavior: for small coupling (large g, where $g \propto 1/\text{coupling}$) the constraint equation has a single solution and the field has no vacuum expectation value (VEV). As one increases the coupling (decreases g) to the "critical coupling" g_{critical}, two additional solutions which give the field a nonzero VEV appear. These solutions differ only infinitesimally from the first solution near the critical coupling, indicating the presence of a second order phase transition. Above the critical coupling ($g < g_{\text{critical}}$), there are three solutions: one with zero VEV, the "unbroken phase," and two with nonzero VEV, the "broken phase". The "critical curves" shown in Figure 7, is a plot of the VEV as a function of g.

5 DLCQ in 3+1 dimensions

Periodic boundary conditions on $\mathcal{L}$ can be realized by periodic boundary conditions on the vector potentials A_μ and anti-periodic boundary conditions on the spinor fields, since $\mathcal{L}$ is bilinear in the Ψ_α. In momentum representation one expands these fields into plane wave states $e^{-ip_\mu x^\mu}$, and satisfies the boundary conditions by *discretized momenta*

$$\begin{aligned} p_- &= \begin{cases} \frac{\pi}{L}n, & \text{with } n = \frac{1}{2}, \frac{3}{2}, \ldots, \infty \quad \text{for fermions,} \\ \frac{\pi}{L}n, & \text{with } n = 1, 2, \ldots, \infty \quad \text{for bosons,} \end{cases} \\ \text{and } \vec{p}_\perp &= \frac{\pi}{L_\perp}\vec{n}_\perp, \qquad \text{with } n_x, n_y = 0, \pm 1, \pm 2, \ldots, \pm\infty \qquad \text{for both.} \end{aligned}$$

As an expense, one has to introduce two artificial length parameters, L and $L_\perp$. They also define the normalization volume $\Omega \equiv 2L(2L_\perp)^2$. More explicitly, the free fields are expanded as

$$\begin{aligned} \widetilde{\Psi}_\alpha(x) &= \frac{1}{\sqrt{\Omega}} \sum_q \frac{1}{\sqrt{p^+}} \left(b_q u_\alpha(p,\lambda) e^{-ipx} + d_q^\dagger v_\alpha(p,\lambda) e^{ipx} \right), \\ \text{and} \quad \widetilde{A}_\mu(x) &= \frac{1}{\sqrt{\Omega}} \sum_q \frac{1}{\sqrt{p^+}} \left(a_q \epsilon_\mu(p,\lambda) e^{-ipx} + a_q^\dagger \epsilon_\mu^\star(p,\lambda) e^{ipx} \right), \end{aligned} \tag{34}$$

particularly for the two transverse vector potentials $\widetilde{A}^i \equiv \widetilde{A}^i_\perp$, $(i = 1, 2)$. As above, each single particle state 'q' is specified by six quantum numbers, the three discrete momenta n, n_x, n_y, helicity, color and flavor. The creation and destruction operators like $a_q^\dagger$ and a_q create and destroy single particle states q, and obey (anti-) commutation relations like

$$[a_q, a_{q'}^\dagger] = \{b_q, b_{q'}^\dagger\} = \{d_q, d_{q'}^\dagger\} = \delta_{q,q'}.$$

The Kronecker symbol is unity only if all six quantum numbers coincide.

Inserting the free fields of Eq.(34) into the Hamiltonian, one performs the space-like integrations and ends up with the light-cone energy-momenta $P^\nu =$

$P^\nu(a_q, a_q^\dagger, b_q, b_q^\dagger, d_q, d_q^\dagger)$ as operators acting in Fock space. The spatial components of P^k are simple and diagonal, the temporal component P^- is complicated and off-diagonal. The integrals over the coordinates x^- are conveiently expressed in Kronecker delta functions

$$\delta(k^+|p^+) = \frac{1}{2L}\int_{-L}^{+L} dx^- e^{+i(k_- - p_-)x^-} = \frac{1}{2L}\int_{-L}^{+L} dx^- e^{+i(n-m)\frac{\pi x^-}{L}} = \delta_{n,m},$$

and correspondingly for the transversal integrations. In the tables given above they appear typically in the overall factor

$$\Delta(q_1; q_2, q_3, q_4) = \frac{g^2}{2\Omega}\,\delta(k_1^+|k_2^+ + k_3^+ + k_4^+)\,\delta^{(2)}(\vec{k}_{\perp 1}|\vec{k}_{\perp 2} + \vec{k}_{\perp 3} + \vec{k}_{\perp 4}).$$

5.1 Retrieving the continuum formulation

The continuum formulation of the Hamiltonian problem in gauge field theory with its endless multiple integrals is usually cumbersome and untransparent. In DLCQ, the continuum limit corresponds to harmonic resolution $K \to \infty$. The compactified formulation with its simple multiple sums is straightforward. The key relation is the connection between sums and integrals

$$\int dk^+ f(k^+, \vec{k}_\perp) \Longleftrightarrow \frac{\pi}{2L}\sum_n f(k^+, \vec{k}_\perp),$$
$$\int d^2\vec{k}_\perp\; f(k^+, \vec{k}_\perp) \Longleftrightarrow \frac{\pi^2}{L_\perp^2}\sum_{n_\perp} f(k^+, \vec{k}_\perp).$$

Combined they yield

$$\int dk^+ d^2\vec{k}_\perp\; f(k^+, \vec{k}_\perp) \Longleftrightarrow \frac{2(2\pi)^3}{\Omega}\sum_{n,n_\perp} f(k^+, \vec{k}_\perp).$$

Similarly, Dirac delta and Kronecker delta functions are related by

$$\delta(k^+)\;\delta^{(2)}(\vec{k}_\perp) \Longleftrightarrow \frac{\Omega}{2(2\pi)^3}\;\delta(k^+|0)\;\delta^{(2)}(\vec{k}_\perp|\vec{0}).$$

Because of that, in order to satisfy the respective commutation relations, one must modify also the creation and destruction operators. Denoting the single boson operators in the continuum by $\widetilde{a}$ and in the discretized case by a, they must be related by

$$\widetilde{a}(q) \Longleftrightarrow \sqrt{\frac{\Omega}{2(2\pi)^3}}\;a_q.$$

and correspondingly for fermion operators. Of course, one has formally to replace sums by integrals, Kronecker delta by Dirac delta functions, and single particle

operators by their tilded versions. In practice, it suffices to replace the tilded coupling constant

$$\widetilde{g}^2 = \frac{g^2}{2\Omega} \qquad \text{by} \qquad \widetilde{g}^2 = \frac{g^2}{4(2\pi)^3}$$

in order to convert the discretized expressions in Tables 1-3 to the continuum formulation.

The DLCQ method can be considered a general framework for solving problems such as relativistic many-body theories or approximate models. The general procedure is: (1) Phrase the physics problem in DLCQ; (2) Apply approximation and simplifications; (3) Derive the final result; (4) At the end convert th so obtained expressions to the continuum.

5.2 Fock-space and vertex regularization

The finite number of Fock-space sectors is a consequence of the positivity of the longitudinal light-cone momentum p^+. The transversal momenta $\vec{p}_\perp$ can take either sign, and the number of Fock states within each sector can be arbitrarily large. In order to face a finite dimensional Hamiltonian matrix one must have a finite number of Fock states, and this is achieved by *Fock space regularization*: Following Lepage and Brodsky [14], a Fock state with n particles is included only if its free invariant mass does not exceed a certain threshold

$$(p_1 + p_2 + \ldots p_n)^2 - (m_1 + m_2 + \ldots m_n)^2 \leq \Lambda_0^2.$$

The sum extends over all n particles in a Fock state. The lowest possible value of M_0^2 is taken when all particles are at rest relative to each other, *i.e.* $(M_0^2)_{min} = (m_1 + m_2 + \ldots m_n)^2$. This frozen invariant mass should be removed from the cut-off The mass scale Λ_0 is a Lorentz scalar and one of the parameters of the theory.

However, it was not realized in the past [8], that Fock-space regularization is almost irrelevant in the continuum theory. *Vertex regularization* seem to be a better alternative. At each vertex, a particle with four-momentum p^μ is scattered into two particles with respective four-momentum p_1^μ and p_2^μ. In order to avoid potential singularities one can *regulate the interaction* by setting the matrix element to zero if the off-shell mass $(p_1 + p_2)^2$ exceeds a certain scale Λ. The condition

$$R(\Lambda) = \Theta\left((p_1 + p_2)^2 - (m_1 + m_2)^2 - \Lambda^2\right) \tag{35}$$

will be referred to as the sharp cut-off for *vertex regularization*.

The dependence on the regularization parameter Λ must be removed by the renormalization group. Renormalization looks like a terrible problem in the context of non-perturbative theory, but with the above regularization scheme it could be simple in principle: The eigenvalues may not depend on the regulator scale(s) Λ. To require this is easier than to find a practical realization.

6 The many-body problem in gauge theory

In principle one proceeds in 3+1 like in 1+1 dimensions: One selects a particular value of the harmonic resolution K and the cut-off Λ and diagonalizes the finite dimensional Hamiltonian matrix by numerical methods. But the bottle neck of any Hamiltonian approach is that the dimension of the Hamiltonian matrix increases exponentially fast with the cut-off. As a concrete example consider the matrix structure as given for $K = 4$ in Fig. 2. Suppose the regularization procedure allows for 10 discrete momentum states in each direction. For every single particle one has about 10^3 possibilities to define a momentum state. A Fock-space sector with n particles and fixed total momentum has then roughly 10^{n-1} different Fock states. Sector 13 in Fig. 2 alone, with its 8 particles, has thus about 10^{21} Fock states. Chemists are able to handle matrices with some 10^7 dimensions, but 10^{21} dimensions exceeds the calculational capacity of any computer in the foreseeable future.

For 3+1 dimensions one is thus confronted with a a similar problem as in conventional many-body physics, displayed in Fig. 3. One has to diagonalize finite matrices with exponentially large dimensions (typically $> 10^6$). In fact, the problem in quantum field theory is even more difficult since the particle number is unlimited. One needs an effective interaction which acts in smaller matrix spaces and which has a well defined relation to the full interaction. One needs it also for the physical understanding. The effective interaction between two electrons, for example, is the Coulomb interaction, at least to lowest order of approximation.

The goal is therefore to develop an exact effective interaction between a quark and an anti-quark in a meson. To achieve this goal, the Hamiltonian DLCQ-matrix is discussed in terms of block matrices, since the Fock-space sectors appear quite naturally in a gauge theory, see also Eq.(18). Each Fock-space sector has a finite number of Fock states, which are kept track of collectively. Eq.(20) is therefore rewritten as a block matrix equation, with $H \equiv H_{LC}$ and $E \equiv M^2$,

$$\sum_{j=1}^{N} \langle i|H|j\rangle \, \langle i|\Psi\rangle = E \, \langle i|\Psi\rangle \qquad \text{for all } i = 1, 2, \ldots, N. \tag{36}$$

Rows and columns are denumerated in the same convention as in Table 7. As to be shown, it can be mapped identically on a matrix equation which acts only in sector $|1\rangle$. Once this is achieved, one can go to the continuum limit.

6.1 The approach of Tamm and Dancoff

Effective interactions are a well known tool in many-body physics [5]. In field theory the method is known as the Tamm-Dancoff-approach, applied first by Tamm [28] and by Dancoff [29], which shall be reviewed it in short.

The rows and columns of a matrix are split into the P- and the Q-space. In terms of the sector numbers of Eq.(36), $P = \sum_{j=1}^{n} |j\rangle\langle j|$ and $Q = \sum_{j=n+1}^{N} |j\rangle\langle j|$,

where $1 \leq n < N$. Eq.(36) can thus be written as a 2 by 2 block matrix equation

$$\begin{aligned} \langle P|H|P\rangle\ \langle P|\Psi\rangle + \langle P|H|Q\rangle\ \langle Q|\Psi\rangle &= E\,\langle P|\Psi\rangle, & (37)\\ \langle Q|H|P\rangle\ \langle P|\Psi\rangle + \langle Q|H|Q\rangle\ \langle Q|\Psi\rangle &= E\,\langle Q|\Psi\rangle. & (38) \end{aligned}$$

If one can invert the quadratic matrix $\langle Q|E-H|Q\rangle$ one could express the Q-space in terms of the P-space wavefunction. But here is a problem: The eigenvalue E is unknown at this point. But one can replace it by another number, *the starting point energy* ω, which is at first a free parameter. The matrix inverse to $\langle Q|\omega - H|Q\rangle$ is called the resolvent of the Hamiltonian in the Q-space and is denoted by $G_Q(\omega)$. The Q-space wave function becomes then

$$\langle Q|\Psi(\omega)\rangle = G_Q(\omega)\langle Q|H|P\rangle\,\langle P|\Psi\rangle, \qquad G_Q(\omega) = \frac{1}{\langle Q|\omega - H|Q\rangle}. \tag{39}$$

Substituting it in Eq.(37) produces an eigenvalue equation in the P-space,

$$H_{\rm eff}(\omega)|P\rangle\,\langle P|\Psi_k(\omega)\rangle = E_k(\omega)\,|\Psi_k(\omega)\rangle, \tag{40}$$

and defines the effective P-space Hamiltonian

$$H_{\rm eff}(\omega) = H + H|Q\rangle\,G_Q(\omega)\,\langle Q|H.$$

Varying ω one generates a set of *energy functions* $E_k(\omega)$. Every solution of the *fix-point equation*

$$E_k(\omega) = \omega,$$

generates one of the eigenvalues H, in fact, it generates all of them.

If one identifies the P- with the $q\bar{q}$-space one seems to have found the effective interaction which acts in the Fock space of a single quark and a single anti-quark. It looks as if one has mapped a difficult problem, the diagonalization of a big matrix onto a simpler problem, the diagonalization of a small matrix. But the price to pay is to invert a matrix. Matrix inversion takes about the same numerical effort as its diagonalization. In view of having to vary ω, the numerical work is therefore rather larger than smaller as compared to a direct diagonalization. The advantage of working with a resolvent is of analytical nature to the extent that resolvents can be approximated systematically. The two resolvents

$$G_Q(\omega) = \frac{1}{\langle Q|\omega - T - U|Q\rangle}, \quad \text{and} \quad \widetilde{G}(\omega) = \frac{1}{\langle Q|\omega - T|Q\rangle}, \tag{41}$$

defined once with and once without the off-diagonal interaction U, are identically related by $G_Q = \widetilde{G} + \widetilde{G}UG_Q$, or by the infinite series of (Tamm-Dancoff) perturbation theory

$$G_Q = \widetilde{G} + \widetilde{G}U\widetilde{G} + \widetilde{G}U\widetilde{G}U\widetilde{G} + \ldots, \tag{42}$$

Sector	n	1	2	3	4	5	6	7	8	9	10	11	12	13
$q\bar{q}$	1	D	S	V	F	·	F	·	·	·	·	·	·	·
$g\ \ g$	2	S	D	V	·	V	F	·	·	F	·	·	·	·
$q\bar{q}\,g$	3	V	V	D	V	S	V	F	·	·	F	·	·	·
$q\bar{q}\,q\bar{q}$	4	F	·	V	D	·	S	V	F	·	·	F	·	·
$g\ \ g\ \ g$	5	·	V	S	·	D	V	·	·	V	F	·	·	·
$q\bar{q}\,g\ \ g$	6	F	F	V	S	V	D	V	·	S	V	F	·	·
$q\bar{q}\,q\bar{q}\,g$	7	·	·	F	V	·	V	D	V	·	S	V	F	·
$q\bar{q}\,q\bar{q}\,q\bar{q}$	8	·	·	·	F	·	·	V	D	·	·	S	V	F
$g\ \ g\ \ g\ \ g$	9	·	F	·	·	V	S	·	·	D	V	·	·	·
$q\bar{q}\,g\ \ g\ \ g$	10	·	·	F	·	F	V	S	·	V	D	V	·	·
$q\bar{q}\,q\bar{q}\,g\ \ g$	11	·	·	·	F	·	F	V	S	·	V	D	V	·
$q\bar{q}\,q\bar{q}\,q\bar{q}\,g$	12	·	·	·	·	·	·	F	V	·	·	V	D	V
$q\bar{q}\,q\bar{q}\,q\bar{q}\,q\bar{q}$	13	·	·	·	·	·	·	·	F	·	·	·	V	D

Table 7: *The Fock-space sectors and the Hamiltonian block matrix structure for QCD. Diagonal blocs are marked by D. Off-diagonal blocks are labeled by V, F and S_6, corresponding to vertex, fork and seagull interactions, respectively. Zero-matrices are denoted by dots. Taken from [32]. See also Fig. 2.*

see also Eq.(21). The free resolvent $\widetilde{G}$ can be obtained trivially since the kinetic energy T is diagonal. Conceptually, it is the same object as the one in Eq.(21), except for two aspects: The present $\widetilde{G}$ acts only in the Q-space, and the starting point energy ω is a *constant* (one of the eigenvalues); the free energy ϵ in (21), however, is a *function of the incoming momenta*. The starting point energy not being a kinetic energy creates problems allover the place, since non-integrable singularities appear in every order of (Tamm-Dancoff) perturbation theory. Essentially two conclusions are possible: Either gauge theory has no bound-state solution, or the series in Eq.(42) has to be resumed to all orders of perturbation theory before the singularities begin cancel eachother.

In practice, Tamm and Dancoff [28, 29] have restricted themselves to the first non-trivial order. In order to make things work, they have replaced the energy denominator with the eigenvalue ω by the energy denominator with the function ϵ, as it appears in the perturbative scattering amplitudes. The same trick was applied in the later work with the front form [30, 31].

Perturbation theory within a bound state problem is known to be a very difficult question. It has motivated the formal work in the next few sections. What we are after is the impossible, some kind of non-perturbative perturbation theory!

6.2 The method of iterated resolvents

The Tamm-Dancoff approach can be interpreted as the reduction of a block matrix dimension from 2 to 1. But having a matrix with block matrix dimension $N = 13$ as in Table 7, it could be interpreted as the reduction from $N \to N-1$, simply by choosing the Q-space appropriately. But then the procedure can be iterated, one can reduce the block matrix dimension from $N-1 \to N-2$, and so on until one arrives at $2 \to 1$. This method of 'iterated of resolvents' has certain advantages, which will be discussed as the formalism develops.

First, one needs a reasonable and compact notation. One of them is to denumerate the Fock space sectors as in Table 7. The full Hamiltonian will be denoted by $H \equiv H_N$, since by the definition in Eq.(36) it has N blocks. Suppose, during the reduction one has arrived at block matrix dimension n, with $1 < n \leq N$. The eigenvalue problem corresponding to Eq.(40) reads then

$$\sum_{j=1}^{n} \langle i|H_n(\omega)|j\rangle\langle j|\Psi(\omega)\rangle = E(\omega)\ \langle i|\Psi(\omega)\rangle, \qquad \text{for } i = 1, 2, \ldots, n.$$

In analogy to Eq.(39), define the n-space resolvent, and get

$$\langle n|\Psi(\omega)\rangle = G_n(\omega) \sum_{j=1}^{n-1} \langle n|H_n(\omega)|j\rangle\ \langle j|\Psi(\omega)\rangle, \quad G_n(\omega) = \frac{1}{\langle n|\omega - H_n(\omega)|n\rangle}. \quad (43)$$

The effective interaction in the $(n-1)$-space becomes then

$$H_{n-1}(\omega) = H_n(\omega) + H_n(\omega)G_n(\omega)H_n(\omega) \quad (44)$$

for every block matrix element. It is unpleasant but unavoidable, that the symbol n denotes both the block matrix dimension and the number of the last sector. Else one proceeds like for Tamm-Dancoff, including the fixed point equation $E(\omega) = \omega$. But one has achieved much more: Eq.(44) is a *recursion relation*!

A few comments seem to be in order. The method of iterated resolvents [32, 33] is particularly suited for gauge theory with its many zero block matrices, see Table 8. The zero matrices remove many of the multiplications in Eq.(43). The Tamm-Dancoff procedure cannot make use of them. – Both the Tamm-Dancoff procedure and the iterated resolvents can be put on a computer in model studies. The iterated resolvents require to invert several smaller matrices insted of one big one. Since matrix diagonalization (and inversion) grows with power 3 in the dimension, the technique of iterated resolvents might thus even be faster. – The iterated and the Tamm-Dancoff resolvents are distinctly different in the following aspect: G_n conserves particle number, but G_Q does not. Both however conserve the incoming momentum. – The notation in Eq.(44) is very compact and will be explained further below. – The method applies also equally well to conventional many-body problems since a pair-interaction generates for example the bloc matrix structure

shown in Figure 3. – Finally, it should be emphasized that the higher sector wavefunctions can be retrieved by matrix multiplications from the eigenfunction in the lowest sector, from $\langle 1|\Psi\rangle$. No additional matrix diagonalizations or inversions are required. To show this, consider Eq.(43) for $n = 1$, *i.e.*

$$\langle 2|\Psi\rangle = \langle 2|G_2H_2|1\rangle\,\langle 1|\Psi\rangle.$$

Both G_2 and H_2 were calculated as a matrix for getting down to the effective interaction in the 1-space. Required is thus one additional matrix multiplication. Next get $\langle 3|\Psi\rangle = \langle 3|G_3H_3|1\rangle\,\langle 1|\Psi\rangle + \langle 3|G_3H_3|2\rangle\,\langle 2|\Psi\rangle$. Substituting $\langle 2|\Psi\rangle$ gives

$$\langle 3|\Psi\rangle = \langle 3|G_3H_3(1 + G_2H_2)|1\rangle\,\langle 1|\Psi\rangle.$$

The general case,

$$\langle n|\Psi\rangle = \langle n|G_nH_n(1 + G_{n-1}H_{n-1})\ldots(1 + G_2H_2)|1\rangle\,\langle 1|\Psi\rangle, \tag{45}$$

can be proven by induction.

6.3 A simple numerical example

It might be interesting to study a Hamiltonian with a tridigonal band structure, such as was given for example in Table 4:

$$\begin{pmatrix} \langle 1|1+S|1\rangle & \langle 1|F|2\rangle & . & . \\ \langle 2|F|1\rangle & \langle 2|1+S|2\rangle & \langle 2|F|3\rangle & . \\ . & \langle 3|F|2\rangle & \langle 3|1+S|3\rangle & \langle 3|F|4\rangle \\ . & . & \langle 4|F|3\rangle & \langle 4|1+S|4\rangle \end{pmatrix}. \tag{46}$$

According to the rules it develops the structure a of continued fraction, since with $G_n(\omega) = 1/(\omega - H_n)$ one has explicitly

$$\begin{array}{llll} H_4 &= \langle 4|1+S|4\rangle, & \langle 4|\Psi\rangle = & \langle 4|G_4FG_3FG_2F|1\rangle\,\langle 1|\Psi\rangle, \\ H_3 &= \langle 3|1+S+FG_4F|3\rangle, & \langle 3|\Psi\rangle = & \langle 3|G_3FG_2F|1\rangle\,\langle 1|\Psi\rangle, \\ H_2 &= \langle 2|1+S+FG_3F|2\rangle, & \langle 2|\Psi\rangle = & \langle 2|G_2F|1\rangle\,\langle 1|\Psi\rangle, \\ H_1 &= \langle 1|1+S+RG_2R|1\rangle, & \langle 1|\Psi\rangle. & \end{array} \tag{47}$$

Here and above a very compact notation is used, which is explained by the example

$$\langle 3|D + VG_4V|3\rangle = \langle 3|D|3\rangle + \langle 3|F|4\rangle\,\langle 4|G_4|4\rangle\,\langle 4|F|3\rangle.$$

By reasons of space, the abbrevation $\langle i|D|i\rangle = \langle i|T + S|i\rangle$ is used sometimes in the diagonal blocks. The kinetic energies T are diagonal matrix elements, and the seagulls do not change particle number by definition. Even that the above is very compact. Here is what it means in terms of matrix operations:

$$\begin{aligned} \langle 3,i|D + FG_4F|3,i'\rangle &= \langle 3,i|D|3,i'\rangle \\ &+ \sum_{j,k}\langle 3,i|F|4,j\rangle\,\langle 4,j|G_4|4,k\rangle\,\langle 4,k|F|3,i'\rangle. \end{aligned}$$

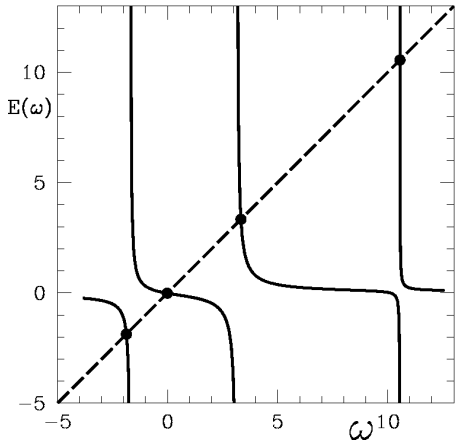

Figure 8: *The the energy function $E(\omega)$ is plotted versus ω. The dotted line represents $E = \omega$.*

The 4×4 matrix

$$\begin{pmatrix} 0 & 1 & . & . \\ 1 & 2 & 3 & . \\ . & 3 & 4 & 5 \\ . & . & 5 & 6 \end{pmatrix}$$

has eigenvalues E_i = -1.872, -0,01518, 3.333, and 10.55. Its energy function is

$$E(\omega) = \cfrac{1 \cdot 1}{\omega - 2 - \cfrac{3 \cdot 3}{\omega - 4 - \cfrac{5 \cdot 5}{\omega - 6}}}.$$

The solutions of $E(\omega) = \omega$ agree with E_i to within computer accuracy. The are marked with $\bullet$ in the figure.

Within each sector $|i\rangle$, the number of basis or Fock states is finite, *i.e.* $|i\rangle \equiv |i; j\rangle$ with $j = 1, 2, \ldots, N_i$. The steps to be taken are then: Take the reactangular block matrix $\langle 4, k|F|1, i'\rangle$; matrix-multiply it from the left with the inverse matrix of $\langle 4|H|4\rangle$ which is $\langle 4, j|G_4|4, k\rangle$; matrix-multiply the result with the transpose (and complex conjugated) matrix $\langle 4, j|F^+|1, i\rangle$; the result is the quadratic matrix $\langle 3, i|FG_4F|3, i'\rangle$; add this to the quadratic matrix $\langle 3, i|D|3, i'\rangle$. As a net result, the old matrix $\langle 3, i|D|3, i'\rangle$ in Eq.(48) is replaced the effective (and ω-dependent) matrix $\langle 1, i|\overline{D}(\omega)|1, i'\rangle$.

To play the game a little further, one can reduce the number of states within a block to 1. Eq.(46) stands then for a tri-diagonal matrix and Eq.(47) stands literally for a continued fraction. Such one is analyzed in Figure 8, with a perfect agreement between the method of iterated resolvents and a direct numerical diagonalization.

6.4 The 4 by 4 block matrix for gauge theory

In the front form, the Fock-space for harmonic resolution $K = 2$ has only 4 Fock-space sectors, see Table 7. $K = 2$ provides thus a good example for all 4 by 4 hermitean bloc matrices, in which the block matrix element $\langle 2|H|4\rangle$ vanishes. The case is considered as an exercise and a non-trivial example.

Since $N = 4$ one starts out with the block matrix

$$\begin{array}{c} \\ 1 = (q\bar{q}) \\ 2 = (gg) \\ 3 = (q\bar{q}\,g) \\ 4 = (q\bar{q}\,q\bar{q}) \end{array} \begin{array}{c} \begin{array}{cccc} 1 = (q\bar{q}) & 2 = (gg) & 3 = (q\bar{q}\,g) & 4 = (q\bar{q}\,q\bar{q}) \end{array} \\ \begin{pmatrix} \langle 1|D|1\rangle & \langle 1|S|2\rangle & \langle 1|V|3\rangle & \langle 1|F|4\rangle \\ \langle 2|S|1\rangle & \langle 2|D|2\rangle & \langle 2|V|3\rangle & 0 \\ \langle 3|V|1\rangle & \langle 3|V|2\rangle & \langle 3|D|3\rangle & \langle 3|V|4\rangle \\ \langle 4|F|1\rangle & 0 & \langle 4|V|3\rangle & \langle 4|D|4\rangle \end{pmatrix} \end{array}. \tag{48}$$

The block matrix element $\langle 2|H_{\rm LC}|4\rangle$ is a rectangular zero-matrix, since the light-cone operator has no matrix elements between two gluons gg and two $q\bar{q}$-pairs. The notation keeps track of the field theoretic property, that each block matrix has only one type of interactions, namely instaneneous seagull (S) and fork (F), or dynamic vertex (V) interactions.

The Hamiltonian in the 4-sector is quadratic and has the resolvent

$$G_4(\omega) = \frac{1}{\langle 4|\omega - H_4|4\rangle}, \qquad \langle 4|H_4|4\rangle = \langle 4|T+S|4\rangle. \tag{49}$$

Using Eq.(44) to reduce the block matrix dimension from 4 to 3 gives

$$\begin{array}{c} \\ 1=(q\bar{q}) \\ 2=(gg) \\ 3=(q\bar{q}\,g) \end{array} \begin{array}{c} \begin{array}{ccc} 1=(q\bar{q}) & 2=(gg) & 3=(q\bar{q}\,g) \end{array} \\ \begin{pmatrix} \langle 1|D+FG_4F|1\rangle & \langle 1|S|2\rangle & \langle 1|(1+FG_4)V|3\rangle \\ \langle 2|S|1\rangle & \langle 2|D|2\rangle & \langle 2|V|3\rangle \\ \langle 3|V(1+G_4F)|1\rangle & \langle 3|V|2\rangle & \langle 3|D+VG_4V|3\rangle \end{pmatrix} \end{array}$$

Almost every block matrix element is replaced by an 'effective' element.

Now continue to reduce from 3 to 2: The resolvent of $\langle 3|H|3\rangle$ is now

$$G_3(\omega) = \frac{1}{\langle 3|\omega - H_3|3\rangle}, \quad \langle 3|H_3|3\rangle = \langle 3|T+S+VG_4V|3\rangle.$$

With $\langle 1|A|1\rangle \equiv \langle 1|T+S+FG_4F+(1+FG_4)VG_3V(1+G_4F)|1\rangle$ one gets

$$\begin{array}{c} \\ 1=(q\bar{q}) \\ 2=(gg) \end{array} \begin{array}{c} \begin{array}{cc} 1=(q\bar{q}) & 2=(gg) \end{array} \\ \begin{pmatrix} \langle 1|A|1\rangle & \langle 1|S+(1+FG_4)VG_3V|2\rangle \\ \langle 2|S+VG_3V(1+G_4F)|1\rangle & \langle 2|T+S+VG_3V|2\rangle \end{pmatrix} \end{array}$$

Finally, evaluate the last resolvent

$$G_2(\omega) = \frac{1}{\langle 2|\omega - H_2|2\rangle}, \quad H_2 = \langle 2|T+S+VG_3V|2\rangle,$$

to end up with the 1 by 1 block matrix

$$\begin{aligned} \langle 1|H_1|1\rangle &= \langle 1|D+FG_4F+(1+FG_4)VG_3V(1+G_4F)|1\rangle \\ &+ \langle 1|(S+VG_3V+FG_4VG_3V)\,G_2\,(S+VG_3V+VG_3VG_4F)|1\rangle. \end{aligned} \tag{50}$$

Here the procedure stops. For gauge theory one can order the result with the power of the coupling constant

$$\begin{aligned} \langle 1|H_1|1\rangle &= \langle 1|T+\overline{VG_3V}+\overline{VG_3VG_2VG_3V}|1\rangle \\ &+ \langle 1|\,SG_2VG_3VG_4F+FG_4VG_3VG_2S+ \\ &\quad VG_3VG_2VG_3VG_4F+FG_4VG_3VG_2VG_3V+ \\ &\quad FG_4VG_3VG_4F+FG_4VG_3VG_2VG_3VG_4F\,|1\rangle. \end{aligned} \tag{51}$$

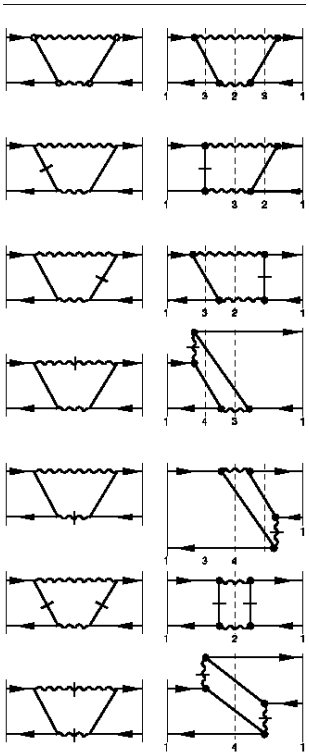

Figure 9: *A particular time-ordering of the two-gluon-annihilation interaction is drawn in the upper left of the figure. If all intrinsic lines are understood as a sum of a 'dynamical' and an ' instantaneous' line, one gets the seven diagrams in the figure, drawn in two different conventions. One observes that the very same strings appear in* $\overline{VG_3VG_2VG_3V}$ *as defined by Eq.(52).*

Figure 10: *Each propagator* G_n *respresents an infinite resummation of Tamm-Dancoff perturbative diagrams. The graph* $\langle 1|VG_3V|1\rangle$ *respresents a resummation of all Tamm-Dancoff graphs with at least one* $q\bar{q}$ *pair, and where a first gluons is emitted by the quark and a (perhaps other) gluon is arbsorbed by the anti-quark.*

with the abbreviations

$$\begin{aligned}
\overline{VG_3V} &= VG_3V + S, \\
\overline{VG_3VG_2VG_3V} &= VG_3VG_2VG_3V + SG_2VG_3V + VG_3VG_2S \\
&+ FG_4VG_3V + VG_3VG_4F + SG_2S + FG_4F. \qquad (52)
\end{aligned}$$

Finally, for completeness, the higher sector wave function in Eq.(45) are written out explicitely

$$\langle 2|\Psi\rangle = G_2\left[\overline{VG_3V} + VG_3VG_4F\right]|1\rangle\langle 1|\Psi\rangle, \qquad (53)$$

$$\langle 3|\Psi\rangle = G_3\left[V + \overline{VG_2VG_3V} + VG_2VG_3VG_4F\right]|1\rangle\langle 1|\Psi\rangle, \qquad (54)$$

$$\langle 4|\Psi\rangle = G_4\left[\overline{\overline{VG_3V}} + \overline{VG_3VG_2VG_3V} + VG_3VG_2VG_3VG_4F\right]|1\rangle\langle 1|\Psi\rangle, \qquad (55)$$

with the additional abbreviations

$$\begin{aligned}
\overline{\overline{VG_3V}} &= VG_3V + F \\
\overline{VG_2VG_3V} &= VG_2VG_3V + VG_4F + VG_2S \\
\overline{\overline{VG_3VG_2VG_3V}} &= VG_3VG_2VG_3V + VG_3VG_4F + VG_3VG_2S. \qquad (56)
\end{aligned}$$

These abbreviations are not very relevant for the general case. But for gauge theory they have a deeper physical meaning as to be discussed further below.

6.5 Discussion and gauge invariant interactions

All effective interactions have a finite number of finite strings like $V\,GV\,\ldots\,GV$. This is a colossal simplification as compared infinite number of terms of Tamm-Dancoff perturbation theory. Iterated resolvents resume them in a systematic way. Both kinds of series can be identified term by term if one expands the iterated resolvents also about the kinetic energies. Denoting the free resolvent by $\widetilde{G}_n$ it is related to the Tamm-Dancoff resolvent $\widetilde{G}$ by

$$\widetilde{G}_n = \sum_{i=1}^{N_n} |n,i\rangle \frac{1}{\omega - T_{n,i}} \langle n,i| \quad , \qquad \widetilde{G}_n = \sum_{n=1}^{N} \widetilde{G}_n$$

If one then expands G_n using $H_n = T_n + U_n$ one gets

$$G_n = \widetilde{G}_n + \widetilde{G}_n U_n \widetilde{G}_n + \widetilde{G}_n U_n \widetilde{G}_n U_n \widetilde{G}_n + \ldots ,$$

thus infinite series of infinite series, which after reordering become identical with the Tamm-Dancoff series.

A look back to Eq.(51) is helpful. The various term have been arranged there by order of the coupling constant. In the first line one finds the combination $\overline{VG_3VG_2VG_3V}$, defined in Eq.(52). In the caption to Figure 9 it is explained how one can simplify the formal procedures, if one associates with each intrisic line a dynamic plus an instantaneous line. Doing that replaces the above sum of six terms into a single one namely $VG_3VG_2VG_3V$, and similarily one replaces the term in the first line by $VG_3V + S \to VG_3V$.

There is a physical reason behind that: When calculating scattering diagrams to a fixed order in perturbation theory, one obtains the gauge invariant Feynman amplitudes only, if all instantaneous graphs of the same order are included. An example for that was given above, when calculating the scattering graph up to second order. Obviously, the method of iterated resolvents accounts for this aspect automatically, in a formal way.

Since the remaining terms in Eq.(51) are of order 6 or 8 in the coupling constant, one concludes that the restriction to the phase space for $K = 2$ satisfies gauge invariance only up to terms of order 6 in the coupling constant. One can verify, that the order of violating gauge invariance is pushed up if one includes more Fock-space sectors. This rule was checked explicitly in many rather laborious calculations in [32].

Theorem 1 *An easy trick to achieve gauge invariance is the following: Set to zero formally all instantaneous interactions, perform the steps required by the resolvents. At the end, when having calculated the effective interaction in terms of the vertex interaction V, one replaces each internal line by the sum of a dynamical and a instantaneous line, according to the general rules of light-cone perturbation theory.*

If one follows thes rules for the 4 by 4 matrix given in Eq.(48) one obtains for the sector Hamiltonians and wavefunctions simply

$$\begin{aligned} H_4 &= T_4, \quad \langle 4|\Psi\rangle = \langle 4|G_4VG_3V + G_4VG_3VG_2VG_3V|1\rangle \langle 1|\Psi\rangle, \\ H_3 &= T_3 + VG_4V, \quad \langle 3|\Psi\rangle = \langle 3|G_3V + G_3VG_2VG_3V|1\rangle \langle 1|\Psi\rangle, \\ H_2 &= T_2 + VG_3V, \quad \langle 2|\Psi\rangle = \langle 2|VG_3V|1\rangle \langle 1|\Psi\rangle, \\ H_1 &= T_1 + VG_3V + VG_3VG_2VG_3V. \end{aligned} \tag{57}$$

These expressions are more transparent than the full equations; they are also gauge invariant.

6.6 The iterated resolvents for arbitrary K

When one substitutes formally all instantaneous interactions by block matrices with only zeros, keeping only the vertex interactions V, one gets a block matrix structure as displayed in Table 8. Because of the many zero matrices, the construction of the the sector Hamiltonians is now rather straightforward and simple. Here they are for the first 12 sectors:

$$H_{12} = T_{12} + VG_{17}V + VG_{17}VG_{16}VG_{12}V + VG_{13}V, \tag{58}$$
$$H_{11} = T_{11} + VG_{16}V + VG_{16}VG_{15}VG_{16}V + VG_{12}V, \tag{59}$$
$$H_{10} = T_{10} + VG_{15}V + VG_{15}VG_{14}VG_{15}V + VG_{11}V, \tag{60}$$
$$H_9 = T_9 + VG_{10}V + VG_{14}V, \tag{61}$$
$$H_8 = T_8 + VG_{12}V + VG_{12}VG_{11}VG_{12}V, \tag{62}$$
$$H_7 = T_7 + VG_{11}V + VG_{11}VG_{10}VG_{11}V + VG_8V, \tag{63}$$
$$H_6 = T_6 + VG_{10}V + VG_{10}VG_9VG_{10}V + VG_7V, \tag{64}$$
$$H_5 = T_5 + VG_6V + VG_9V, \tag{65}$$
$$H_4 = T_4 + VG_7V + VG_7VG_6VG_7V, \tag{66}$$
$$H_3 = T_3 + VG_6V + VG_6VG_5VG_6V + VG_4V, \tag{67}$$
$$H_2 = T_2 + VG_3V + VG_5V, \tag{68}$$
$$H_1 = T_1 + VG_3V + VG_3VG_2VG_3V, \tag{69}$$

Actually, for $K = 4$, the exact expressions corresponding to Table 8 are obtained by setting $G_{13} = 1/(\omega - T_{13})$ and $G_n = 0$ for $n \geq 14$. But it is easy to write down the expressions in Eqs.(58)-(60) valid for a higher value of K. One also notes that they give all sector Hamiltonians for $K = 2$ in Eqs.(57), by setting formally $G_n = 0$ for $n \geq 5$.

Theorem 2 *For sufficiently large harmonic resolution K the formal expressions for effective Hamiltonian in sufficiently low sectors become independent of K.*

One therefore can go to the limit $K \to \infty$ and thus to the continuum limit.

Sector	n	1	2	3	4	5	6	7	8	9	10	11	12	13
$q\bar{q}$	1	D	·	V	·	·	·	·	·	·	·	·	·	·
$g\ \ g$	2	·	D	V	·	V	·	·	·	·	·	·	·	·
$q\bar{q}\,g$	3	V	V	D	V	·	V	·	·	·	·	·	·	·
$q\bar{q}\,q\bar{q}$	4	·	·	V	D	·	·	V	·	·	·	·	·	·
$g\ \ g\ \ g$	5	·	V	·	·	D	V	·	·	V	·	·	·	·
$q\bar{q}\,g\ \ g$	6	·	·	V	·	V	D	V	·	·	V	·	·	·
$q\bar{q}\,q\bar{q}\,g$	7	·	·	·	V	·	V	D	V	·	·	V	·	·
$q\bar{q}\,q\bar{q}\,q\bar{q}$	8	·	·	·	·	·	·	V	D	·	·	·	V	·
$g\ \ g\ \ g\ \ g$	9	·	·	·	·	V	·	·	·	D	V	·	·	·
$q\bar{q}\,g\ \ g\ \ g$	10	·	·	·	·	·	V	·	·	V	D	V	·	·
$q\bar{q}\,q\bar{q}\,g\ \ g$	11	·	·	·	·	·	·	V	·	·	V	D	V	·
$q\bar{q}\,q\bar{q}\,q\bar{q}\,g$	12	·	·	·	·	·	·	·	V	·	·	V	D	V
$q\bar{q}\,q\bar{q}\,q\bar{q}\,q\bar{q}$	13	·	·	·	·	·	·	·	·	·	·	·	V	D

Table 8: *The Fock space and the Hamiltonian matrix $H' = T + V$ for a meson at fixed value of $K = 4$. — See discussion in the text. The diagonal blocks are denoted by T. Most of the block matrices are zero matrices, marked by a dot $(\cdot)$. The block matrices marked by V are potentiall non-zero due to the vertex interaction.*

6.7 Propagation in medium

Here seems to be a problem: For calculating G_3 one needs G_6, G_5 and G_4, for calculating G_6 one needs G_{10}, G_9 and G_7, and so on. In the next section will be shown how the hierarchy can be broken in a rather effective way. That final step will be comparatively simple if one has analyzed the propagators for the sectors with one $q\bar{q}$-pair and arbitrarily many gluons, as follows next.

Consider first the the effective interaction in the space of one $q\bar{q}$-pair and one gluon as given by Eq.(67). The corresponding diagrams can be grouped into two topologically distinct classes, displayed in Figs. 12 and 13. The the diagrams in Fig. 12 are obtained by adding a non-interacting gluon line to the former diagrams in Fig. 11. The gluon does not change quantum numbers under impact of the interaction and acts like a spectator. Therefore, the graphs in Fig. 12 will be refered to as the 'spectator interaction' $\overline{U}_3$. In the graphs of Fig. 13 the gluons are scattered by the interaction, and correspondingly these graphs will be refered to as the 'participant interaction' $\widetilde{U}_3$. Thus, $U_3 = \overline{U}_3 + \widetilde{U}_3$. The separation into a graph with only one interacting quark-pair Fock-space sectors

$$U_n = \overline{U}_n + \widetilde{U}_n, \tag{70}$$

except in those with only gluons. More explicitly, the spectator and participant

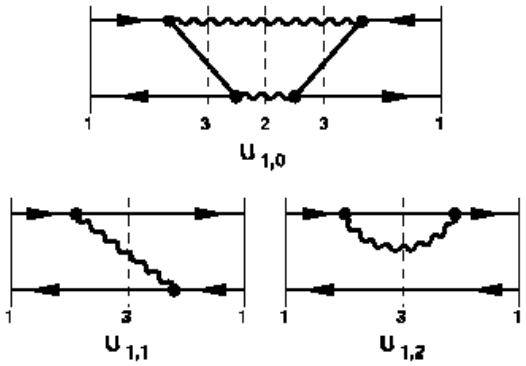

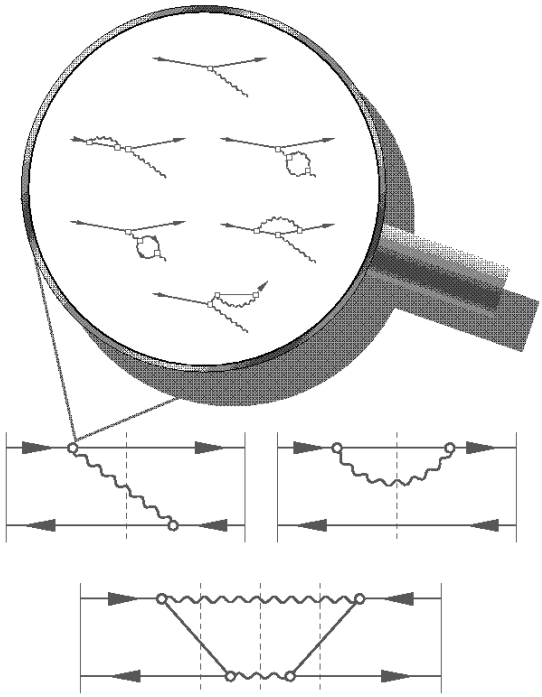

Figure 11: *The three graphs of the effective interaction in the $q\bar{q}$-space. The vertical lines denote the propagators G_n. On the right, the vertical lines denote the propagators $\overline{G}_n$. The coupling function at the vertices is symbolized by graphs as they would appear in a perturbative analysis.*

interactions in the lowest sectors with one quark-pair become

$$\begin{array}{rclcl} \overline{U}_3 & = & VG_6V & + & VG_6VG_5VG_6V, \\ \overline{U}_6 & = & VG_{10}V & + & VG_{10}VG_9VG_{10}V, \end{array} \qquad \begin{array}{rclcl} \widetilde{U}_3 & = & VG_4V & + & VG_6V, \\ \widetilde{U}_6 & = & VG_7V & + & VG_{10}V. \end{array} \tag{71}$$

The same operators can appear in both $\overline{U}$ and $\widetilde{U}$, but they refer to different graphs. Since the Hamiltonian is additive in spectator and participant interactions, $\overline{U}_n$ can be associated with its own resolvent

$$\overline{G}_n = \frac{1}{\omega - T_n - \overline{U}_n}, \qquad \Big(\text{while } G_n \equiv \frac{1}{\omega - H_n} = \frac{1}{\omega - T_n - \overline{U}_n - \widetilde{U}_n}\Big). \tag{72}$$

The relation of $\overline{G}_n$ to the full resolvent is $G_n = \overline{G}_n + \overline{G}_n\,\widetilde{U}_n\,G_n$, or

$$G_n = \overline{G}_n + \overline{G}_n\widetilde{U}_n\,\overline{G}_n + \overline{G}_n\widetilde{U}_n\,\overline{G}_n\widetilde{U}_n\,\overline{G}_n + \ldots, \tag{73}$$

writing it as an infinite series. Note that the propagator $\overline{G}_n$ contains the interaction $\widetilde{U}_n$ in contrast to the free Tamm-Dancoff propagator $\widetilde{G}$ in Eq.(41). One deals here therefore with 'perturbation theory in medium'. But since it is driven to all orders one better speaks of 'propagation in medium'.

The series can be identically written as

$$G_n = C_n\,\overline{G}_n\,C_n^\dagger, \qquad \text{with} \quad C_n = \sqrt{\frac{1}{1 - \overline{G}_n\widetilde{U}_n}}. \tag{74}$$

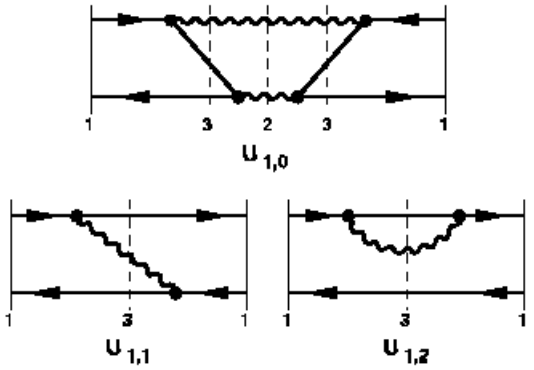

Figure 12: *The three graphs of the spectator interaction in the $q\bar{q}\,g$-space. Note the role of the gluon as a spectator.*

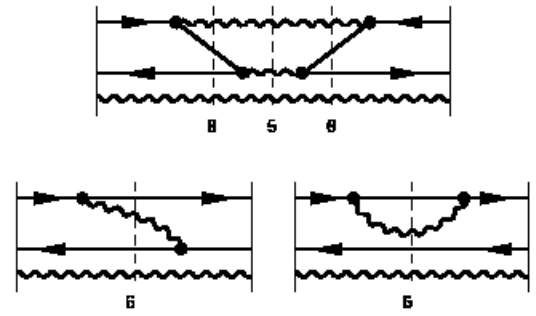

Figure 13: *Some six graphs of the participant interaction in the $q\bar{q}\,g$-space.*

One can verify this order by order in perturbation theory or by the identity

$$(\omega - \overline{H}_n)(1 - \overline{G}_n \widetilde{U}_n) = (\omega - \overline{H}_n)\left(1 - \frac{1}{\omega - \overline{H}_n}\widetilde{U}_n\right) = \omega - H_n. \tag{75}$$

The inverse gives $C_n^2\,\overline{G}_n = G_n$, and with the identity $C_n\,\overline{G}_n = \overline{G}_n\,C_n^\dagger$, one gets Eq.(74). This remarkable property is peculiar to the method of iterated resolvents. Whenever a quark-pair-glue resolvent is sandwiched in between two vertex interactions, it allows to define a modified vertex interaction $\overline{V}$, since

$$V\,G_n\,V^\dagger = V\,C_n\,\overline{G}_n\,C_n^\dagger\,V^\dagger = \overline{V} G_n\,\overline{V}^\dagger, \text{ with } \quad \overline{V} = VC_n. \tag{76}$$

One can thus rewrite the sector Hamiltonians like for example

$$\overline{U}_6 = \overline{V}\,\overline{G}_{10}\overline{V} + \overline{V}\,\overline{G}_{10}\overline{V}G_9\overline{V}\,\overline{G}_{10}\overline{V}, \tag{77}$$

$$\overline{U}_3 = \overline{V}\,\overline{G}_6\overline{V} + \overline{V}\,\overline{G}_6\overline{V}G_5\overline{V}\,\overline{G}_6\overline{V}, \tag{78}$$

$$U_1 = \overline{V}\,\overline{G}_3\overline{V} + \overline{V}\,\overline{G}_3\overline{V}G_2\overline{V}\,\overline{G}_3\overline{V}. \tag{79}$$

Now they have all essentially the same structure, contrary to Eqs.(69) where they were different. Note that G_2, G_5 and G_9 are pure gluon propagators.

Generally spoken, the rectangular block matrix V is multiplied with the square matrix C_n. Below it will be shown that C_n is approximately diagonal and independent of the spin. Each vertex matrix element is multiplied with a simple function which depends on the momentum transfer Q across the vertex. Equivalently one replaces the coupling constant g by $\overline{g} = gC_n(Q)$, such that C_n can be interpreted as a *coupling function.*

6.8 The exact effective interaction

The most important result of this section is that gauge theory particularly QCD has only two structurally different contributions to the effective interaction in the $q\bar{q}$-space, see Eq.(79). It scatters a quark with helicity λ_q and four-momentum $p = (xP^+, x\vec{P}_\perp + \vec{k}_\perp, p^-)$ into a state with λ'_q and four-momentum $p' = (x'P^+, x'\vec{P}_\perp + \vec{k}'_\perp, p'^-)$, and correspondingly the antiquark. In the *continuum limit*, the resolvents are replaced by propagators and the matrix eigenvalue problem $H_{\rm eff}|\psi\rangle = M^2|\psi\rangle$ becomes an integral equation with a rather transparent structure:

$$M_i^2\langle x,\vec{k}_\perp;\lambda_q,\lambda_{\bar{q}}|\psi_i\rangle = \left[\frac{\overline{m}_q^2+\vec{k}_\perp^2}{x}+\frac{\overline{m}_{\bar{q}}^2+\vec{k}_\perp^2}{1-x}\right]\langle x,\vec{k}_\perp;\lambda_q,\lambda_{\bar{q}}|\psi_i\rangle \tag{80}$$

$$+\sum_{\lambda'_q,\lambda'_{\bar{q}}}\int dx'd^2\vec{k}'_\perp\; R(x',k'_\perp)\,\langle x,\vec{k}_\perp;\lambda_q,\lambda_{\bar{q}}|U_{\rm OGE}|x',\vec{k}'_\perp;\lambda'_q,\lambda'_{\bar{q}}\rangle\,\langle x',\vec{k}'_\perp;\lambda'_q,\lambda'_{\bar{q}}|\psi_i\rangle$$

$$+\sum_{\lambda'_q,\lambda'_{\bar{q}}}\int dx'd^2\vec{k}'_\perp\; R(x',k'_\perp)\,\langle x,\vec{k}_\perp;\lambda_q,\lambda_{\bar{q}}|U_{\rm TGA}|x',\vec{k}'_\perp;\lambda'_q,\lambda'_{\bar{q}}\rangle\,\langle x',\vec{k}'_\perp;\lambda'_q,\lambda'_{\bar{q}}|\psi_i\rangle.$$

The domain of integration is set by the cut-off function R given in Eq.(35). The effective one-gluon exchange

$$U_{\rm OGE} = \overline{VG}_3\overline{V} \tag{81}$$

conserves the flavor along the quark line. As illustrated in Fig. 11 the vertex interaction V creates a gluon and scatters the system virtually into the $q\bar{q}\,g$-space. As indicated in the figure by the vertical line with subscript '3', the three particles propagate there under impact of the full Hamiltonian before the gluon is absorbed. The gluon can be absorbed either by the antiquark or by the quark. If it is absorbed by the quark, it contributes to the effective quark mass $\overline{m}$. The second term in Eq.(79) is the effective two-gluon-annihilation interaction,

$$U_{\rm TGA} = \overline{VG}_3\overline{V}G_2\overline{VG}_3\overline{V}, \tag{82}$$

as represented by the graph $U_{1,0}$ in Fig. 11. The virtual annihilation of the $q\bar{q}$-pair into two gluons can generate an interaction between different quark flavors. – The eigenvalue M_i^2 is one of the invaraint-mass squared eigenvalues of the full light-cone Hamiltonian, and the wavefunction $\langle x,\vec{k}_\perp;\lambda_q,\lambda_{\bar{q}}|\psi_i\rangle$ gives the probability amplitudes for finding in the $q\bar{q}$-state a flavored quark with momentum fraction x, intrinsic transverse momentum $\vec{k}_\perp$ and helicity λ_q, and correspondingly an antiquark with $1-x$, $-\vec{k}_\perp$ and $\lambda_{\bar{q}}$.

7 The breaking of the propagator hierarchy

The content of the preceeding sections is exact but rather formal. In the sequel, rigor will be given up by the aim to obtain a solvable equation. In order to spot

easier the essential approximations, they will be dressed as 'theorems', which can – or cannot – be proven later.

All sector Hamiltonians can be diagonalized on their own merit, for example

$$\begin{aligned} M^2_{1;i}\,\langle q;\bar q|\Psi_{1;i}\rangle &= \sum_{q',\bar q'}\langle q;\bar q|H_1|q';\bar q'\rangle\,\langle q';\bar q'|\Psi_{1;i}\rangle, \\ M^2_{3;i}\,\langle q;\bar q;g|\Psi_{3;i}\rangle &= \sum_{q',\bar q',g'}\langle q;\bar q;g|\overline{H}_3|q';\bar q';g'\rangle\,\langle q';\bar q';g'|\Psi_{3;i}\rangle. \end{aligned} \tag{83}$$

The spectra might be continuous, but the eigenvalues are denumerated for simplicity by i. By construction, one knows the relation between these two sets of eigenvalues, by the following reason: Because of the separation into spectators and participants the gluon in the $q\bar q\,g$-equation is a non-interacting particle. it moves freely relative to a $q\bar q$-bound state. If its four-momentum is parametrized as $q^\mu = (yP^+, y\vec P_\perp + \vec q_\perp, q_g^-)$ one has

$$M^2_{3;i} = \frac{M^2+\vec q_\perp^{\,2}}{(1-y)} + \frac{\vec q_\perp^{\,2}}{y}. \tag{84}$$

Every $q\bar q$ bound state M is a band-head in the $q\bar q\,g$ spectrum. With $\omega = M^2_{1,0}(\omega) \equiv M^2$ one gets

$$\omega - M^2_{3;i} = M^2 - \left(\frac{M^2_{1;0}+\vec q_\perp^{\,2}}{(1-y)} + \frac{\vec q_\perp^{\,2}}{y}\right) = -\frac{y^2M^2+\vec q_\perp^{\,2}}{y(1-y)}. \tag{85}$$

Knowing the eigenvalues and the eigenfunctions of the $q\bar q$ bound state one alos know the spectrum and the eigenfunctions of $\overline{H}_3$. Knowing the eigenfunctions, the exact resolvent can be calculated.

Theorem 3 *The exact propagators can be approximated by closure.*

The substitution of the exact propagators by closure is a widely used approximation in many-body theory and in chemistry. In principle, the exact propagator is non-diagonal. Performing closure, it becomes diagonal, which is reflected by the Dirac-delta function $\langle q;\bar q;g|q';\bar q';g'\rangle$ in the single particle momenta and helicities

$$\langle q;\bar q;g|\overline{G}_3|q';\bar q';g'\rangle = \langle q;\bar q;g|q';\bar q';g'\rangle\overline{G}_3(q;\bar q;g). \tag{86}$$

The Dirac-delta function is multiplied with the function

$$\overline{G}_3(q;\bar q;g) = -\frac{y(1-y)}{y^2M^2+\vec q_\perp^{\,2}}. \tag{87}$$

The in-medium propagator $\overline{G}_3$ ceases to be a functional of the higher resolvents. *The hierarchy of the iterated resolvents is broken.*

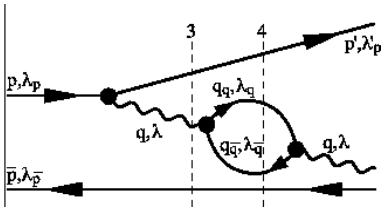

Figure 14: *The $q\bar{q}$ vacuum polarization graph.*

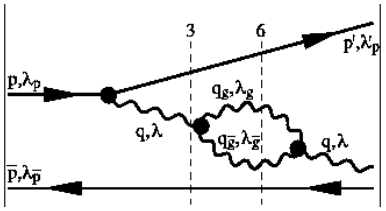

Figure 15: *The gg vacuum polarization graph.*

Theorem 4 *In the solution, the interacting particles propagate free particles. The in-medium propagators can be replaced by the free propagators.*

The free propagator in the $q\bar{q}g$-space can be written

$$G_{3,\text{free}} = \frac{1}{P^+(p^- - p'^- - q^-)} = -\frac{y}{Q^2} = -\frac{y}{y^2(2\overline{m})^2 + \vec{q}_\perp^{\,2}}, \tag{88}$$

where $Q^2 = (p-p')^2$ is the four-momentum transfer along the quark line, in the notation of Fig. 14. For sufficiently small y holds $(p-p')^2 = -[y^2(2\overline{m})^2 + \vec{q}_\perp^{\,2}]$. If one substitutes $M \simeq 2\overline{m}$, which holds to rather good approximation, the momentum transfer in Eq.(88) is the same as in Eq.(87).

Similar considerations also hold all other propagators with at least one $q\bar{q}$-pair.

Having replaced the in-medium-propagators $\overline{G}_n$ by the free propagators, one can calculate the graphs like in the usual (light-cone-) time-ordered perturbation theory. The diagram $U_{1,2}$ in Fig. 11 yields the effective quark mass

$$\overline{m}_f^2 = m_f^2 + m_f^2 \frac{\alpha}{\pi} \frac{n_c^2 - 1}{2n_c} \ln \frac{\Lambda^2}{m_g^2}. \tag{89}$$

Correspondingly one can calculate the coupling function

$$C_3 = \sqrt{\frac{1}{1 - \overline{G}_3 \widetilde{U}_3}} = 1 + \frac{1}{2}\overline{G}_3\widetilde{U}_3 + \frac{3}{8}\overline{G}_3\widetilde{U}_3\,\overline{G}_3\widetilde{U}_3 + \ldots, \tag{90}$$

as defined by Eq.(74). With $\widetilde{U}_3 = VG_4V + VG_6V$ from Eq.(71), and thus $\widetilde{U}_3 = \overline{VG_4V} + \overline{VG_6V}$ from Eq.(76), the first two terms in the expansion are

$$\overline{V} \simeq V + \frac{1}{2}(V\overline{G}_3\overline{VG_4V} + V\overline{G}_3\overline{VG_6V}) \simeq V + \frac{1}{2}(V\overline{G}_3V\overline{G}_4V + V\overline{G}_3V\overline{G}_6V). \tag{91}$$

In the last step $R_4 = R_6 = 1$ was set. In general, they contribute terms of higher orders in g, which must be suppressed for consistency. Figs. 14 and 15 give only 2 representative graphs. According to the rules of time ordered perturbation theory, there are about 22 different time-ordered and instantaneous diagrams. All of them

were re-calculated by Raufeisen [34], for all values of Q. As shown to some detail in [33] one gets for sufficiently large Λ

$$\begin{aligned}\overline{G}_3 V(\overline{G}_6+\overline{G}_4)V &= \frac{11\alpha n_c}{12\pi}\ln\left(\frac{\Lambda^2}{4m_g^2+Q^2}\right)-\frac{\alpha}{6\pi}\sum_f \ln\left(\frac{\Lambda^2}{4m_f^2+Q^2}\right),\\ &= \alpha\, b_0 \ln(\Lambda^2/\kappa^2)-b(Q), \quad b_0=\frac{11n_c-2n_f}{12\pi}, \end{aligned} \tag{92}$$

with an arbitrary κ and a $b(Q)$ independent of Λ given in Eq.(93). One conculdes that the coupling function C_3 is identical with the familiar vertex correction. In the limit where Q is larger than all mass scales, this result agrees with the calculations of both, Thorn [35] and Perry [36], having been done previously.

What happens if one substitutes the free propagators in Eq.(90) by the non-perturbative propagators $\overline{G}_4=(\omega-\overline{H}_{q\bar{q}\,q\bar{q}})^{-1}$ and $\overline{G}_6=(\omega-\overline{H}_{q\bar{q}\,gg})^{-1}$, at least in an approximate fashion? — There are additional graphs. In the fermion loop of vacuum polarization appear two graphs in addition to Fig. 14. In one of them, a gluon is emitted and absorbed on the same quark line which changes the bare quark mass m_f into the physical quark mass $\overline{m}_f$. In the other graph, the gluon is emitted from the quark and absorbed by the anti-quark which represents an interaction. In consequence one has a bound state with a physical mass scale μ_f. We replace therefore $2m_f \Longrightarrow 2\overline{m}_f \Longrightarrow \mu_f$. Similar considerations hold for the gluon loop in Fig. 15 and lead to the substitution $2m_g \Longrightarrow 2\overline{m}_g \Longrightarrow \mu_g$. Both μ_g and μ_f are interpreted as physical mass scales. The physical gluon mass $\overline{m}_g$ vanishes of course due to gauge invariance. This is not in conflict with *f.e.* Cornwall's suggestion of a finite effective gluon mass [37] since one can define $(\overline{m}_g)_{\rm eff}\equiv\mu_g/2$.

As a consequence of the approximation in Eq.(86), the propagators $\overline{G}_3$ and $\overline{G}_4$ are diagonal in Fock space, which in turn leads to diagonal products $\overline{G}_3 V \overline{G}_4 V$. They can be resumed therefore to all orders according to Eq.(90). With $\overline{\alpha}\equiv g^2C_3^2/4\pi$, one gets

$$\begin{aligned}\overline{\alpha}(Q;\Lambda) &= \frac{1}{1/\alpha-b_0\ln(\Lambda^2/\kappa^2)+b(Q)} \quad \text{with}\\ b(Q) &= \frac{11n_c}{12\pi}\ln\Big(\frac{\kappa^2}{\mu_g^2+Q^2}\Big)-\frac{1}{6\pi}\sum_f\ln\Big(\frac{\kappa^2}{\mu_f^2+Q^2}\Big). \end{aligned} \tag{93}$$

The effective fine structure constant depends on the momentum transfer Q across the vertex and on the cut-off Λ. Now, all the pieces are together which are needed for a further discussion of the effective interaction as defined in Eq.(80). Finally, the the instantaneous interaction in the effective one-gluon-exchange interaction $U_{OGE}=\overline{VG}_3\overline{V}$ is restored according to $\overline{VG}_3\overline{V}\longrightarrow C_3^2(V\overline{G}_3V+S)$, with the expression given in Eq.(26).

8 Status and discussion

What have we reached? – The general expression for the effective Hamiltonian in the $q\bar{q}$-sector was given in Eq.(80). If one restricts to consider mesons in which the quark and the anti-quark have different flavors, $f_q \neq f_{\bar{q}}$, the two-gluon annihilation diagram can not get active and one remains with

$$M_n^2\langle x,\vec{k}_\perp;\lambda_q,\lambda_{\bar{q}}|\psi_n\rangle = \left[\frac{\overline{m}_q^2(\Lambda)+\vec{k}_\perp^2}{x}+\frac{\overline{m}_{\bar{q}}^2(\Lambda)+\vec{k}_\perp^2}{1-x}\right]\langle x,\vec{k}_\perp;\lambda_q,\lambda_{\bar{q}}|\psi_n\rangle$$
$$+\sum_{\lambda_q',\lambda_{\bar{q}}'}\int dx'd^2\vec{k}_\perp'\ \langle x,\vec{k}_\perp;\lambda_q,\lambda_{\bar{q}}|U_{\rm OGE}|x',\vec{k}_\perp';\lambda_q',\lambda_{\bar{q}}'\rangle\ \langle x',\vec{k}_\perp';\lambda_q',\lambda_{\bar{q}}'|\psi_n\rangle \quad . \quad (94)$$

The essential achievement of the two preceeding sections is that the kernel of this integral equation can be written down in the very explicit form

$$\langle\lambda_q,\lambda_{\bar{q}}|U_{\rm OGE}|\lambda_q',\lambda_{\bar{q}}'\rangle = -\frac{\overline{\alpha}(Q;\Lambda)}{3\pi^2Q^2}\,\langle\lambda_q,\lambda_{\bar{q}}|S|\lambda_q',\lambda_{\bar{q}}'\rangle\frac{R(x',k_\perp';\Lambda)}{\sqrt{x(1-x)x'(1-x')}}. \quad (95)$$

All many-body effects reside in the effective mass $\overline{m}_q(\Lambda)$ and in the effective coupling constant $\overline{\alpha}(Q;\Lambda)$. They are given in Eqs.(89) and (93), respectively. The mean of the four-momentum transfers of quark and anti-quark, $Q_q^2=-(k_q-k_q')^2$ and $\overline{Q}_{\bar{q}}^2=(k_{\bar{q}}-k_{\bar{q}}')^2$, respectively, is denoted by Q^2. The spinor factor is

$$\langle\lambda_q,\lambda|S|\lambda_q',\lambda'\rangle = [\overline{u}(k,\lambda)\gamma^\mu u(k',\lambda')]_q\ [\overline{u}(k,\lambda)\gamma_\mu u(k',\lambda')]_{\bar{q}}\,.$$

The cut-off function R sets the domain of integration and is defined in Eq.(35). The approximations made have been carefully enumerated in Section 7.

One has thus reached the goal of reducing the field theoretical many-body problem of $M^2 = H_{\rm LC}$ to a one-body problem with an effective interaction. For any value of the Lagrangian coupling constant g, the flavor masses m_f, and the cut-off Λ, one can generate the eigenvalues M_n^2 on a computer, very much in analogy to QED [30, 31]. With the known eigenfunction in the $q\bar{q}$-sector one an generate all higher Fock-space amplitudes, according to the explicit formulas in Section 6. It looks as if one has solved the problem.

But one has solved the problem only in a superficial way, since the solutions depend on the unphysical parameter Λ. One of the central issues in gauge-field theory is to remove this dependence by a renormalization group analysis, see below.

The eigenvalues of the integral equation are the invariant masses squared. Very often it is more convenient to think in terms of an analogue of a non-relativistic Hamiltonian H_S,

$$H_{\rm LC} = (\overline{m}_{\bar{q}}+\overline{m}_{q'})^2 + 2(\overline{m}_{\bar{q}}+\overline{m}_{q'})\ H_S, \quad (96)$$

whose eigenvalues $E = H_S$ are the more convential binding energies, while the eigenfunctions are the same. As shown in [2], the so defined 'Schrödinger operator' has much in common with a non-relativistic Hamiltonian for the Coulomb problem.

8.1 Renormalization group analysis

All eigenvalues M_n^2 depend thus on the cut-off Λ, the bare masses m and the bare α. In line with modern interpretation of quantum field theory [7], they are unphysical parameters and can be replaced by $(m_\Lambda, \alpha_\Lambda)$, by functions of Λ, such that the eigenvalues are cut-off independent, *i.e.*

$$\frac{d}{d\Lambda} M_n^2(\Lambda, \alpha_\Lambda, m_\Lambda) = 0. \tag{97}$$

This fundamental equation of the renormalization group must hold for all eigenvalues.

The effective Hamiltonian $H = H_{\rm LC,eff}$ depends on Λ only through $\overline{m}_f$, $\overline{\alpha}$ and the regulator function R. The renormalization group equations can be written therefore in the operator form

$$\delta\overline{m}_f \frac{\delta H}{\delta \overline{m}_f}|\psi_n\rangle + \delta\overline{\alpha}\frac{\delta H}{\delta\overline{\alpha}}|\psi_n\rangle + \delta R \frac{\delta H}{\delta R}|\psi_n\rangle = 0. \tag{98}$$

The simultaneous variation of all three terms is a very difficult problem. But one can replace this equation by three independent ones,

$$\frac{d}{d\Lambda}\overline{m}_f = 0, \tag{99}$$

$$\frac{d}{d\Lambda}\overline{\alpha} = 0, \tag{100}$$

$$\frac{dR}{d\Lambda}\frac{\delta H}{\delta R}|\psi_n\rangle = 0. \tag{101}$$

This is possible since one still solves Eq.(98).

Eqs.(99) and (100) are two equations for the two unknown functions m_Λ and α_Λ. The first equation says that the effective flavor masses $\overline{m}_f = \overline{m}_f(\Lambda, \alpha_\Lambda, m_\Lambda)$ are renormalization group invariants. The numerical value of $\overline{m}_f$ must be fixed by experiment. – Eq.(100) is then considered as an equation for α_Λ at fixed values of $\overline{m}_f$. Using the expression for $\overline{\alpha}(Q;\Lambda)$ given in Eq.(93) yields then [33]

$$\alpha_\Lambda = \frac{1}{b_0 \ln\left(\Lambda^2/\kappa^2\right)}, \quad \text{thus} \quad \overline{\alpha}(Q) = \frac{1}{b(Q)}, \tag{102}$$

with $b(Q)$ given in Eq.(93). All Λ-dependence cancels exactly in favor of the renormalization group invariant κ, which is sometimes called the QCD-scale $\Lambda_{\rm QCD}$. The scale κ must be determind from experiment. – Once α_Λ is known, Eq.(99) is an equation for m_Λ. This function can be determined from Eq.(89), but we renounce to do that here, since m_Λ is needed nowhere in the present context. – Having fixed the functions α_Λ and m_Λ one has exhausted all freedom provided by conventional renormalization anaysis of field theory [7]. Since the cutoff-dependence was removed by renormalization, the cut-off can be driven to infinity, thus

$$R(x, \vec{k}_\perp; \Lambda) = 1.$$

Formally, this solves Eq.(101).

8.2 The remaining divergence

After renormalization, the kernel of the one-body equation is independent of Λ. Let us discuss its relevant part

$$\mathcal{K} = \frac{1}{b(Q)} \frac{S}{Q^2}.$$

At very small momentum transfers $Q^2 \to 0$, where $x \sim x'$ and $\vec{k}_\perp \sim \vec{k}'_\perp$, the effective coupling constant locks into the finite value $b(0)$, see Eq.(93). The spinor function also goes to a constant, $S \sim 4\overline{m}_q \overline{m}_{\bar{q}}$, see [31] or [2]. The remaining 'Coulomb singularity' Q^{-2} is square-integrable and can be dealt with by convenient numerical means [30, 31]. For very large momentum transfers $Q^2 \to \infty$, the behaviour is quite different. Both S and Q^2 tend to diverge, $S \propto (\vec{k}'_\perp)^2$ and $Q^2 \propto (\vec{k}'_\perp)^2$, but such that the ratio S/Q^2 tends to a *finite constant*. Disregarding the very slow logarythmic increase of $b(Q)$, the kernel of the integral equation is therefore essentially a dimensionless constant

$$\mathcal{K} \sim constans, \qquad \text{for} \quad Q^2 \gg 0.$$

One has sufficient evidence [31] that this behaviour creates all kinds of problems, among them a diverging eigenvalue.

One can separate the kernel of the integral equation identically into two pieces $\mathcal{K} = \mathcal{K}_1 + \mathcal{K}_2$, *i.e.*

$$\mathcal{K} = \frac{1}{b(Q)} \frac{S}{Q^2} \frac{\mu^2 + Q^2}{\mu^2 + Q^2} = \frac{1}{b(Q)} \frac{S}{Q^2(1 + Q^2/\mu^2)} + \frac{S}{b(Q)(\mu^2 + Q^2)},$$

with an arbitrary mass parameter μ. The first part $\mathcal{K}_1$ is well behaved and vanishes at least like Q^{-2} in the limit of large Q. The second part $\mathcal{K}_2$ is a strange object: it is a constant almost everywhere, in particular

$$\mathcal{K}_2 \sim constans, \qquad \text{since} \quad \frac{S}{Q^2} \sim constans, \qquad \text{for} \quad Q^2 \gg 0.$$

One should emphasize the following aspect. The typical field theoretical divergences like the divergence of the effective coupling constant lead to a *divergence* of the kernel, but adding a *finite constant* to the kernel leads also to a divergence. Thus far one does not understand the reason for the latter.

Perhaps one can get further insight by studying the following eigenvalue in (usual) three-momentum space ($\vec{k}$)

$$E\psi(\vec{k}) = \frac{\vec{k}^{\,2}}{2m}\psi(\vec{k}) - \frac{\alpha}{\pi^2} \int d^3k' \left[\frac{1}{(\vec{k} - \vec{k}')^2} + \frac{1}{\mu^2} \right] \psi(\vec{k}'). \tag{103}$$

In the spirit of Eq.(96), the right-hand side is a conventional Schrödinger equation for the Coulomb problem with the reduced mass $1/m = 1/m_q + 1/m_{\bar{q}}$, but where an

	$\overline{u}$	$\overline{d}$	$\overline{s}$	$\overline{c}$	$\overline{b}$
u		768	892	2007	5325
d	140		896	2010	5325
s	494	498		2110	—
c	1865	1869	1969		—
b	5278	5279	5375	—	

	$\overline{u}$	$\overline{d}$	$\overline{s}$	$\overline{c}$	$\overline{b}$
u		ρ^+	K^{*+}	$\overline{D}^{*0}$	B^{*+}
d	π^-		K^{*0}	D^{*-}	B^{*0}
s	K^-	$\overline{K}^0$		D_s^{*-}	B_s^{*0}
c	D^0	D^+	D_s^+		B_c^{*+}
b	B^-	$\overline{B}^0$	$\overline{B}_s^0$	B_c^-	

Table 9: *The empirical masses of the flavor-off-diagonal physical mesons in MeV. Vector mesons are given in the upper, pseudo-scalar mesons in the lower triangle. Their physical nomenclature is given on the right.*

	$\overline{u}$	$\overline{d}$	$\overline{s}$	$\overline{c}$	$\overline{b}$
u		^{*768}	902	2012	5331
d	^{*140}		902	2012	5331
s	^{*494}	494		2155	5476
c	^{*1865}	1865	2108		6617
b	^{*5278}	5278	5423	6573	

	$\overline{u}$	$\overline{d}$	$\overline{s}$	$\overline{c}$	$\overline{b}$
u		^{*768}	1002	2301	5696
d	^{*140}		1002	2301	5696
s	^{*494}	494		2535	5829
c	^{*1865}	1865	2102		7227
b	^{*5278}	5278	5512	6811	

Table 10: *The calculated masses of the flavor-off-diagonal mesons in MeV, as obtained from a fit to Eq.(105) on the left and to Eq.(104) on the right. Vector mesons are given in the upper, pseudo-scalar mesons in the lower triangle. The *upperscript marks mesons where the shift and mass parameters have be fitted to.*

arbitrary constant has been added in the kernel. In Heidelberg, we are presently working on the question whether its eigenvalue E diverges. Preliminary studies with the Fourier transform of Eq.(103), where the constant works its way into a weird Dirac-delta function $\delta^{(3)}(\vec{x})$ as a potential,

$$E\phi(\vec{x}) = -\frac{\vec{\nabla}^2}{2m}\phi(\vec{x}) - \left[\frac{\alpha}{|\vec{x}|} + \frac{\alpha}{\mu^2}\delta^{(3)}(\vec{x})\right]\phi(\vec{x}'),$$

indicate indeed that the eigenvalue of the $1s$-state in particular diverges.

If these preliminary results materialize, one must regularize and subsequently renormalize Eq.(103). The energy of the $1s$-state will then be essentially a renormalization constant $E_{1s} = \overline{s}$. Given that to be true, all of us have been riding the wrong horse. It is not the regular part of the interaction kernel $\mathcal{K}_1$, but it is the 'constant' $\mathcal{K}_2$ which determines the mass in the first place. Since $\mathcal{K}_2$ involves a renormalization and since the singlet can have an energy shift ($\overline{s}_-$) different from the triplet ($\overline{s}_+$), one has at most two additional renormalization constants, subject to be determined by experiment.

method	$\overline{m}_u$	$\overline{m}_d$	$\overline{m}_s$	$\overline{m}_c$	$\overline{m}_b$	$\overline{s}_-$	$\overline{s}_+$
Eq.(104)	350	350	583	1881	5275	-336	71
Eq.(105)	350	350	495	1637	4972	-336	71

Table 11: *The quark mass parameters $\overline{m}_q$ and the energy shifts $\overline{s}_\pm$, all in MeV, as obtained from a fit to the physical meson masses.*

8.3 A mass formula

Is there some physical evidence for the above considerations? – Inspired by Eq.(96), one can seek the masses of the physical mesons in the form [38]

$$M^2 = (\overline{m}_{\bar{q}} + \overline{m}_{q'})^2 + 2(\overline{m}_{\bar{q}} + \overline{m}_{q'})\ \overline{s}_\pm, \tag{104}$$

and fit the energy shifts $\overline{s}_\pm$ and the physical quark masses $\overline{m}_q$ to the physical meson masses, compiled in Table 9 from the data of the particle data group [39] which do not include yet the topped mesons.

The following procedure was applied. First, the up and the down mass were chosen equal. Then the empirical masses of π^+ and ρ^+ were used to determine the mass shifts for the singlet and the triplet. The remaining quark masses are obtained from the pseudo-scalar mesons with an up quark, which exhausts all freedom in determining physical parameters. The remaining 13 off-diagonal pseudo-scalar and vector meson masses are calculated straightforwardly and compiled in Table 10. In comparing the so obtained numbers with the experiment, one notes with great surprise that the discrepancy exceeds only rarely an estimated error of 10%. The resulting quark masses are given in Table 11.

Actually, there is no reason why one should stick to Eq.(104). Equivalently, one can replace $\overline{s}_\pm$ by $\overline{s}_\pm\, a/(\overline{m}_{\bar{q}} + \overline{m}_{q'})$. Choosing $a = \overline{m}_{\bar{u}} + \overline{m}_d = 700$ MeV, one gets

$$M^2 = (\overline{m}_{\bar{q}} + \overline{m}_{q'})^2 + 2(\overline{m}_{\bar{u}} + \overline{m}_d)\ \overline{s}_\pm. \tag{105}$$

A form like this was suggested to me by Dae Sung Hwang during the lectures. Redoing the fit for the heavy quarks gives the results compiled in Table 10. The discrepancy with the experimental numbers is now on the level of 1%. This excellent agreement should not be over-emphasized. In any case it does not falsify the above considerations.

9 A short summary

In these lecture notes the attempt was made to phrase and discuss a relativistic quantum theory such as QCD from the point of view of Dirac's front form of

hamiltonian dynamics. Sometimes refered to as light-cone quantization, it has the goal to describe and understand the bound-state structure of hadrons in terms of their constituents from a covariant theory. As the lectures show, this goal has not been reached yet.

As reviewed in [2], there might be alternative roads to reach the same goal, like for example the Bethe-Salpeter equations, lattice gauge theory, Hamiltonian flow equations, just to name a few. Each of these approaches have their own inherent adventages or disadventages. By reasons of space their discussion is left out in these notes. By the same reason the light-front renormalizations approach of Wilson and collaborators [40, 41] is omitted. The many articles have thus far not provided conclusive evidence for success, apart from the fact that virtually every Langrangian symmetry has been violated in the approach. It is much too early to draw definitive conclusions.

The front form is however useful to study the structure of arbitrary field theories. The theories considered are often not physical, but are selected to help in the understanding of a particular non-perturbative phenomenon. The relatively simple vacuum properties of light-front field theories underly many of these 'analytical' approaches. The relative simplicity of the light-cone vacuum provides a firm starting point to attack many non perturbative issues. As we have seen, the problems in two dimensions, in one space and one time dimension, not only are they tractable from the outset but in many cases like the Schwinger model can they be solved numerically by 'discretized light-cone quantization (DLCQ)' to almost arbitrary accuracy. This solution gives a unique insight and understanding. The Schwinger particle indeed has the simple parton structure that one hopes to see in QCD.

Unfortunately the same cannot be said for the physical world in 3 space and 1 time dimensions. The essential problem is that the number of degrees of freedom needed to specify each Fock state even in a discrete basis grows much too quickly. As discussed in this review, the basic procedure is to diagonalize the full light-cone Hamiltonian in the free light-cone Hamiltonian basis. The eigenvalues are the invariant mass squared of the discrete and continuum eigenstates of the spectrum. The projection of the eigenstate on the free Fock basis are the light-cone wavefunctions and provide a rigorous relativistic many-body representation in terms of its particle degrees of freedom. Given the light-cone wavefunction one can compute the structure functions and distribution amplitudes. More generally, the light-cone wavefunctions provide the interpolation between hadron scattering amplitudes and the underlying parton subprocesses. The method of iterated resolvents can be a useful intermediary step to generate these wavefunctions. The unique property of light-cone quantization that makes the calculations of light cone wavefunctions particularly useful is that they are independent of the reference frame and that the same wavefunction can be use in many different problems.

Finally, let us highlight the intrinsic advantages of light-cone field theory:

- The light-cone wavefunctions are independent of the momentum of the bound state – only relative momentum coordinates appear.
- The vacuum state is simple and in many cases trivial.
- Fermions and fermion derivatives are treated exactly; there is no fermion doubling problem.
- The minimum number of physical degrees of freedom are used because of the light-cone gauge. No Gupta-Bleuler or Faddeev-Popov ghosts occur and unitarity is explicit.
- The output is the full color-singlet spectrum of the theory, both bound states and continuum, together with their respective wavefunctions.

References

[1] P.A.M. Dirac, Rev. Mod. Phys. **21**, 392 (1949).

[2] S.J.Brodsky, H.C. Pauli, S.S. Pinsky, Physics Reports **301**, 299-486 (1998).

[3] A. Bassetto, G.Nardelli and R. Soldati, *Yang-Mills Theories in Algebraic Non-covariant Gauges* (World Scientific,Singapore, 1991).

[4] J.D. Bjørken and S.D. Drell, *Relativistic Quantum Mechanics* (McGraw-Hill, New York, 1964); J.D.Bjørken and S. D. Drell, *Relativistic Quantum Fields* (McGraw-Hill,NewYork, 1965).

[5] P.M. Morse and H. Feshbach, *Methods in Theoretical Physics*, 2 Vols, (Mc Graw-Hill, New York, N.Y., 1953).

[6] T. Muta, *Foundations of Quantum Chromodynamic*. Lecture notes in Physics, Vol.5 (World Scientific, Singapore, 1987).

[7] S. Weinberg, *The quantum theory of fields*, 2 Vols, (Cambridge University Press, New York, 1995).

[8] S.J. Brodsky and H.C. Pauli, in *Recent Aspect of Quantum Fields*, H. Mitter and H. Gausterer, Eds.; Lecture Notes in Physics,Vol. 396 (Springer-Verlag, Berlin, Heidelberg, 1991).

[9] F. Coester, Prog. Nuc. Part. Phys. **29**, 1 (1992).

[10] *Theory of Hadrons and Light-front QCD*, S. Glazek, Ed., (World Scientific Publishing Co., Singapore, 1995).

[11] *New non-perturbative methods and quantization on the light cone*, P. Grangé, A. Neveu, H.C. Pauli, S. Pinsky and E. Werner, Eds., (Springer Verlag, Berlin, Heidelberg, 1997).

[12] W. Lucha, F.F. Schöberl, and D. Gromes, Physics Reports **200**, 127 (1991).

[13] J.B. Kogut and D.E. Soper, Phys. Rev. **D1**, 2901 (1970).

[14] G.P. Lepage and S.J. Brodsky, Phys. Rev. **D22**, 2157 (1980).

[15] H.C. Pauli, Z. Phys. **A319**, 303 (1984).

[16] H.C. Pauli and S.J. Brodsky, Phys. Rev. **D32**, 1993 (1985); **D32**, 2001 (1985).

[17] T. Eller, H.C. Pauli and S.J. Brodsky, Phys. Rev. **D35**, 1493 (1987).

[18] K. Hornbostel, S. J. Brodsky and H. C. Pauli, Phys. Rev. **D41**, 3814 (1990).

[19] D.P. Crewther and C.J. Hamer, Nucl. Phys. **B170**, 353 (1980).

[20] H. Bergknoff, Nucl. Phys. **B122**, 215 (1977).

[21] T. Eller and H.C. Pauli, Z. Physik **C42**, 59 (1989).

[22] S. Elser, Proceedings of *Hadron structure '94*, Kosice, Slowakia (1994); and Diplomarbeit, U. Heidelberg (1994).

[23] M. Völlinger, Diplomarbeit, U. Heidelberg (1996).

[24] J.P. Vary, T.J. Fields and H.-J. Pirner, Phys. Rev. **D53**, 7231-7238 (1996).

[25] B. van de Sande, Phys. Rev. **D54**, 6347 (1996). hep-ph/9605409.

[26] T. Maskawa and K. Yamawaki, Prog. Theor. Phys. **56**, 270 (1976).

[27] S.S. Pinsky and B. van de Sande, Phys. Rev. **D49**, 2001 (1994).

[28] I. Tamm, J. Phys. (USSR) **9**, 449 (1945).

[29] S.M. Dancoff, Phys. Rev. **78**, 382 (1950).

[30] M. Krautgärtner, H.C. Pauli and F. Wölz, Phys. Rev. **D45**, 3755 (1992).

[31] U. Trittmann and H.C. Pauli, "Quantum electrodynamics at strong coupling", Heidelberg preprint MPI H-V4-1997, Jan. 1997. hep-th/9704215

[32] H.C. Pauli, in: *Neutrino mass, Monopole Condensation, Dark matter, Gravitational waves and Light-Cone Quantization*, B.N. Kursunoglu, S. Mintz and A. Perlmutter, Eds., (Plenum Press, New York, 1996) p.183-204; hep-th/9608035, hep-th/9707361, Heidelberg preprint MPIH-V9-1998, Mar. 1998.

[33] H.C. Pauli, Eur.Phys.J.**C7**, 289 (1998); hep-th/9809005, hep-th/9608035.

[34] J. Raufeisen, Diplomarbeit (in German), Universität Heidelberg (1997).

[35] C.B. Thorn, Phys. Rev. **D19**, 639 (1979); Phys. Rev. **D20**, 1934 (1979).

[36] R.J. Perry, A. Harindranath, and W.M. Zhang, Phys. Lett. **B300**, 8 (1993).

[37] J.M. Cornwall and A. Soni, Phys.Lett. **120B**, 431 (1983).

[38] H.C. Pauli, Preprint MPIH-V15-1999, Preprint MPIH-V16-1999.

[39] C. Caso *et al.* (Particle Data Group), Eur.Phys.J. **C3**, 1 (1998).

[40] K.G. Wilson, T.S. Walhout, A. Harindranath, W.M. Zhang, R.J. Perry, S.D. Głazek, Phys. Rev.**D49**, 6720 (1994).

[41] S.D. Glazek and K.G. Wilson, Phys. Rev.**D57**, 3558 (1998).